FAST BREEDER REACTORS

5509

W. Häfele
AND
D. Faude, E. A. Fischer, H. J. Laue
Kernforschungszentrum Karlsruhe, Germany

CONTENTS

Introduction

The principle of breeding has been recognized from the very beginning of the development of nuclear reactors. Realizing that the η value, which characterizes the average number of neutrons produced by fission per absorbed neutron ($(n, \gamma)+(n, f)$), is high for fast neutrons inducing the fission process, Fermi & Zinn began to design a fast breeder reactor as early as 1944 (1). This was the beginning of a first round of fast breeder development, lasting from 1944 until roughly 1960, leading to reactors that are often referred to as fast breeders of the first generation. The US reactors EBR-I, EBR-II, EFFBR, the British DFR, and the Russian BR-5 are the more prominent of these reactors (see Table 1) (2–8).

Consistent with the general approach to reactor technology of these early years the principal fuel was metal, more specifically U metal (9). Interconnected to that was the choice of Na as the principal coolant. The cores were small, the Na temperatures modest, and the breeding mostly external, i.e. the margin appeared in the reflecting blanket and not so much in the core directly. With respect to long-term reactor strategies the main attention was given to the doubling time (9, 10); core inventory and fuel cycle costs were not in the forefront of interest to the same extent. All of these factors had certain consequences for the way in which the problems were attacked.

Around 1960, economic considerations with the background of a maturing thermal reactor technology led to a shift of attention to the fuel cycle as a whole (11). In particular it became clear that the burnup of the fuel must be increased if economic feasibility is to be achieved. A natural uranium reactor, for instance, requires a burnup of only ~7000 MWd/ton to burn effectively all original fissionable atoms. Fast reactors inherently require

high enrichment, and burnups of ~100,000 MWd/ton are required in order to keep the number of passes of an individual fissionable atom through the full fuel cycle to tolerable level. To achieve these required high burnups, in 1960 considered almost frightening, it was mainly UO_2 or UO_2/PuO_2 that offered the best chance.

This led to what is now often referred to as the second generation of fast breeders. The paper of Sampson & Luekbe (12) was the first step. Following that, it was particularly the groups of General Electric (GE) (13) and Karlsruhe (14) that pursued this new direction. After the IAEA conference in Vienna (15) this ceramic fast reactor scheme received worldwide attention together with the shift of emphasis from breeding to economy (16).

It became apparent that the reactor design would differ somewhat from that of the first generation because of neutron moderation by the oxygen atoms in the UO_2/PuO_2 fuel. At first, then, most attention was concentrated on calculating the Doppler coefficient (17, 18). This led to major undertakings such as the SEFOR reactor (19, 20), which was specifically designed to measure and demonstrate the Doppler coefficient during various sorts of fast-reactor transients. The possibilities for a measurement of the Doppler coefficient in a critical zero-power facility also were explored and finally understood in the early sixties.

After it was realized that the Doppler coefficient would be sufficiently negative, the next point of interest was the Na void effect (21)—the reactivity change that occurs after fully or partly voiding the core of Na, and turns out to be positive for sufficiently large fast cores (18), which caused major concern in the fast-reactor community. The four large 1000 MW*e* design studies of General Electric, Westinghouse, Combustion Engineering, and Babcock and Wilcox concentrated to a very large extent on this problem (22). Among other things these studies revealed that demanding all power coefficients to be negative was too restrictive.

Related to these problems is the question of the target size of a reference fast reactor. In the first fast-reactor generation the considered sizes were very small, up to 150 MW*e* or so, but during the early sixties it became clear that much larger reactor stations must be envisaged. Most, but not all the aspects of fast-reactor design become easier as the size of the core increases, because the necessary fraction of fissile atoms in the fuel goes down. Between 1959 and 1963, 500 MW*e* was often considered to be a good target size (23), but after the above-mentioned four design studies in the US, and other studies (24), 1000 MW*e* was generally accepted as a target value for realistic fast-reactor designs.

By means of the power coefficients these questions are interrelated to inherent fast-reactor safety. At the Argonne Conference of 1965 the various then existing fast-reactor reference designs (25) were analyzed with respect to possible chains of events that could lead to a major accident. It became apparent that the Na void effect becomes important only if a very unlikely type of major accident takes place, for instance the malfunction of the shut-

off system or Na boiling effects. Therefore the whole problem of Na void was put into the realm of more hypothetical accidents and the core designs accordingly could be more conventional, as it was then no longer necessary to reduce the Na void effect at almost any cost. Along the same lines it was recognized that a series of other phenomena also require the same degree of attention as the Na void effect, for instance Na boiling and superheating, as this may be responsible for the time scale of a Na voiding (26–28). This evolution of thinking led towards engineered safeguards and away from too much emphasis on inherent safety.

It coincided timewise (1966–1967) with the first results of high burnup pin irradiations. The first high burnup of ~70,000–80,000 MWd/ton was obtained in thermal reactors such as GETR at Vallecitos and others, but pins, which had been irradiated particularly at DFR and EBR-II, followed. They all indicated good results, provided that the density of the mixed oxide fuel is low enough. From that it was generally concluded that 50,000 MWd/ton would be a good starting value for the performance of a first fast core of a prototype. So most fast-reactor groups of the world decided to take the step of building a 300 MW*e* Na-cooled early prototype.

Long-range strategic considerations had revealed the desirability of having a 1000 MW*e* fast breeder power station by 1980 (29, 30). The original target date of the US fast breeder development was much later, as late as 1989 (31), but fast breeders should be available from 1980 on, in order to have a large breeder capacity for the year 2000 and thereby to reduce the demand for too much uranium ore. Breeding will be a necessity only after the year 2000, but in order to have it at that time on a large scale the first reactors must be introduced by 1980.

Another fairly strong argument was forwarded by K. P. Cohen (32) and others: The unexpected large-scale installation of light-water reactors (LWR) leads to a large production of Pu. If Pu is being recycled into these LWR, its value as compared with ^{235}U would be only something like 80% of that of ^{235}U while introduction of the Pu into a fast reactor gives a value of roughly 140% (33). In other words, fast reactors can stand a high Pu price and therefore there is a natural partnership between LWRs and fast breeders.

Along these two lines of argument the UK was the first in the West to go ahead with her 250 MW*e* plutonium-fueled fast reactor PFR at Dounreay (34), France pushed the design of her 250 MW*e* PHENIX prototype (35), and Germany together with Belgium, the Netherlands, and Luxembourg that of their 300 MW*e* SNR reactor (36). American industry and in particular General Electric, Westinghouse, and Atomics International (AI) opted for the same approach with the same basic argument: If such a 300 MW*e* prototype were built around 1970 or a little earlier, it would give sufficient time to let a 600 MW*e* or 1000 MW*e* plant follow, which ultimately would demonstrate the commercial availability of fast breeders with Na cooling (37). In Russia the design and construction of the BN-350 (38) was going on and at least timewise this Russian group was and still is in the lead for this class of pro-

totype reactors. In Table 2 more details are given for these prototype reactors, or, as they are called in the US, *demonstration reactors*.

Sodium technology must be duly mastered and cheap enough, if the utilities all over the world are to rely on it. The question of reliability, availability, and capital cost of these Na components is therefore under constant discussion and investigation. Also some more recent results on the behavior of structural materials such as stainless steel after having been exposed to high fast-neutron doses ($>10^{22}$ *nvt*) and high fluxes ($>2\cdot10^{15}$ n/cm^2 sec) indicated reasons for concern as unexpected swelling phenomena in these materials occurred. Further, the approach of engineered safeguards requires among other things in-core instrumentation. So it is not surprising that there is another voice in the US, pressing more for the large-scale fast-neutron test reactor FFTF in order to have an orderly procedure in the design and the development of fast breeders, even if this leads to some time delay (39, 40).

Large fast breeder reactors of 1000 MW*e* using a ceramic fuel instead of metallic fuel also allow for coolants other than Na. The large size of 1000 MW*e* brings the fraction of fissile atoms down to something like 12% as compared with 25% or higher in the first generation of fast breeders; this is one factor 2. The small density of UO_2/PuO_2 fast reactor fuel as compared with the density of metallic fuel in the first generation gives another factor 2. Therefore the power density in such a large fast ceramic reactor is lower by at least a factor 4 as compared with the early concept of the first generation. This explains in principle the additional degree of freedom with respect to the coolant. A number of groups therefore considered dry steam as a fast-reactor coolant (41, 42). The general idea was to extrapolate the established and proven LWR technology to the fast breeders. The breeding ratio is of course lower, but still clearly above 1, and the whole approach looked promising. This idea was ultimately dropped because the fuel pin design presented difficulties whose main components were a large external pressure on the cladding, dry-steam corrosion attack, and the necessity for tight lattices and high temperatures. The dry-steam, fast-reactor fuel pin required a broad fuel testing and this in turn required a test bed for such fuel with dry steam as a coolant. Such a test bed was not available and was finally considered too expensive and time consuming (43). The same requirement for proper test beds in case of the Na-cooled fast reactor did of course also exist, but it was filled by the reactors of the early first generation. EBR-II, DFR, BR-5 and for some time also EFFBR were used for such irradiation performance tests. Today no group pursues the line of a steam-cooled fast reactor.

There is some recent interest in He as a fast-reactor coolant (44–46). Helium-cooled fast breeder reactors also require excessive fuel pin testing in a proper environment and therefore again a proper test bed. This again leads to the problem of a test reactor, this time for He as a coolant, and introduces time delays as compared with the Na (47). But contrary to the dry-steam idea it seems to be clear that such a He-cooled fast reactor has a long-range

potential if very high temperatures and possibly a direct He turbine cycle are used (48, 49). Therefore from this different angle the question of a large fast test reactor again becomes the focus of attention (37).

Finally, the present Na-cooled fast-reactor line using UO_2/PuO_2 indeed does not require, as we saw, a fast test reactor as a test bed for the necessary fuel pin development, but the long-range potential of the Na-cooled reactor lies beyond the present UO_2/PuO_2 fuel and requires high neutron fluxes. Therefore the development of Na coolant also ultimately requires such a test reactor. Along this line of argument the Karlsruhe group is developing plans for a fast test reactor FR-3 with Na cooling and a number of test loops capable of handling other coolants such as He also (50). The concepts of the US FFTF reactor and the German FR-3 turn out to be very similar, at least in the present stage.

So the overall picture shows in most cases a line of development that leads to prototype reactors of the 300 MW*e* class, all scheduled around 1970 for the start of construction and around 1974 for completion. Russia and Great Britain are already preparing for the next step, a 600 MW*e* fast breeder. Complementary to that is the line of development in the US that makes the FFTF the major milestone, and a similar reactor, FR-3, is being prepared in Germany for somewhat different reasons. To make the picture complete it should be mentioned that Italy has decided to build first a somewhat small but versatile test reactor PEC as a starting point for a possible future evolution (51), and India is considering the construction of an experimental fast reactor. Japan on the other hand has decided to make the development of a Na-cooled fast breeder reactor a major national project. Their development is about 3 or 4 years behind the European developments, but it is a very well coordinated effort, well funded and fully self-consistent (52, 53).

As mentioned before, Tables 1, 2, and 3 illustrate the above broad picture. It should be mentioned here that an alternative approach to breeding in a thermal reactor is being pursued at Oak Ridge, where the molten salt breeder reactor concept is under development using the thorium-^{233}U fuel cycle. The successful operation of an experimental reactor, the MSRE (Molten Salt Reactor Experiment), which first became critical in 1965, demonstrated that the concept of a fuel which is dissolved in molten fluoride salts is feasible. The fuel is being circulated during operation, and reprocessing is performed in a small on-site plant. In October 1969 the MSRE became the world's first reactor to operate on ^{233}U. This concept is still in an early stage of development; it is judged that it might become economically attractive by the end of the century. Returning to the main line of fast breeders, we now will review the various areas of fast breeder development in more detail.

Fast-Reactor Physics

Among the main reasons for distinguishing between the first- and the second-generation fast breeder are their neutron spectra, and Doppler and Na void coefficients.

TABLE 1. First-generation fast breeder reactors

		USA				USSR			UK	France
		CLEMENTINE	EBR-I	EBR-II	EFFBR	BR-1	BR-2	BR-5	DFR	RAPSODIE
Reactor power										
Thermal	MW*t*	0.025	1.2	62.5	200	0	0.1	5	72	20
Electrical	MW*e*	0	0.2	20	66	0	0	0	15	0
Core										
Fuel		Pu metal	U metal	U metal	U metal	Pu metal	Pu metal	PuO_2	U metal	PuO_2/UO_2
Core volume	liters	2.5	6	65	420	1.7	1.7	17	120	54
Fuel rating av	MW*t*/kg fiss	0.0016	0.02	0.3	0.37	0	0.008	0.1	0.24	0.14
Power density av	MW*t*/liter	0.01	0.17	0.8	0.45	0	0.06	0.3	0.5	0.32
Linear rod power max	W/cm	(av 50)	300	450	250	0	150	200	(av 320)	(av 210)
Neutron flux max	n/cm² sec	(av $5 \cdot 10^{12}$)	$1.1 \cdot 10^{14}$	$3.7 \cdot 10^{15}$	$4.7 \cdot 10^{15}$	$5 \cdot 10^{10}$	$1 \cdot 10^{14}$	$1 \cdot 10^{15}$	$2.5 \cdot 10^{15}$	$1.8 \cdot 10^{15}$
Primary heat-transfer system										
Coolant		Hg	NaK	Na	Na	—	Hg	Na	NaK	Na
Coolant temperature										
Core inlet	°C	40	230	370	290	—	30	375	200	410(450)
Core outlet	°C	120	320	470	430	—	60	450(500)	350	500(540)
Coolant mass flow	m³/h	0.6	80	2200	5500	—	6	240	1800	800
Number of coolant loops		1	1	2	3	—	1	2	24	2
Time schedule										
Design		1945	1945					1956		1958
Construction		9/1946	1949	1957	8/1956			1957	3/1955	1962
First criticality		11/1946	8/1951	10/1961	8/1963			6/1958	11/1959	1/1967
Full operation		3/1949	12/1951	4/1965	8/1966	1955	1956	7/1959	7/1963	3/1967
Shutdown		6/1953	1963	—	—	1956	1957	—	—	—
Remarks		First fast reactor, First Pu-fueled reactor	First nuclear electricity generation Pu-core since 1962	Reactor plant with integral fuel processing facility	Since 10/1966 out of operation			UC-core since 1965		(RAPSODIE is not really a reactor of the first generation, it belongs to a large extent to the second generation)

TABLE 2. Second-generation fast breeder reactors

		USA			USSR		UK	France	Germany
		GE	WESTINGHOUSE	AI	BN-350	BN-600	PFR	PHENIX	SNR
Reactor power									
Thermal	MW*t*	750	770	1250	1000	1470	600(670)	563	730
Electrical	MW*e*	310	300	500	350	600	250(275)	250	300
Core (reference)									
Fuel		PuO_2/UO_2	PuO_2/UO_2	PuO_2/UO_2	PuO_2/UO_2 or UO_2	PuO_2/UO_2	PuO_2/UO_2	PuO_2/UO_2	PuO_2/UO_2
Core volume		2000	1960	3000	1900	2300	1320	1150	1600
Fuel rating av	MW*t*/kg fiss	0.82	0.85	0.9	0.96		0.7	0.8	0.8
Power density av	MW*t*/liter	0.31	0.39	0.37	0.5	0.6	0.4	0.42	0.4
Linear rod power	max W/cm	500	440	490	470		450	430	400
Breeding ratio		1.2	1.22	1.3	1.5		1.2	1.16	1.29
Burnup	MWd/ton	100,000	75,000	75,000	50,000	100,000	70,000	50,000	55,000
Primary heat-transfer system									
Type		Pool	Loop	Loop	Loop	Pool	Pool	Pool	Loop
Coolant		Na	Na	Na	Na	Na	Na	Na	Na
Number of coolant loops		3	2	3	5	3	3	3	3
Pump capacity	m^3/h	5000	8500	8850	3200	9300	5000	4800	5100
Coolant temperature									
Core inlet	°C	425	400	405	300	380	400–425	400(420)	380
Core outlet	°C	590	550	570	500	530	560–585	560(580)	550
Steam conditions									
Temperature	°C	510	480	480	435	505	510–540	510	505
Pressure	at	160	170	163	50	140	162	167	165
Date of operation		(1975)	(1975)	(1975)	1970		1971/72	1973	1975

TABLE 3. Second-generation experimental fast reactors

		USA		USSR	France	Germany	Italy	Japan
		SEFOR	FFTF	BOR-60	RAPSODIE fortissimo	KNK-II	PEC	JEFR
Reactor power								
Thermal	MW*t*	20	400	60	40	58	130	100
Electrical	MW*e*	0	0	12	0	20	0	0
Core								
Fuel		PuO_2/UO_2	PuO_2/UO_2	PuO_2/UO_2 or UO_2	PuO_2/UO_2	PuO_2/UO_2 $+UO_2$	UO_2	PuO_2/UO_2
Core volume	liter	500	1030	53	45	320	420	280
Linear rod power max	W/cm	650	500	590	400	430	400	430
Neutron flux max	n/cm²sec	$6 \cdot 10^{14}$	$7{,}2 \cdot 10^{15}$		$3 \cdot 10^{15}$	$2{,}3 \cdot 10^{15}$	$2{,}8 \cdot 10^{15}$	$4 \cdot 10^{15}$
Primary heat-transfer system								
Type		Loop	Loop		Loop	Loop	Loop	Loop
Coolant		Na	Na	Na	Na	Na	Na	Na
Number of coolant loops		1		2	2	2	2	2
Coolant temperature								
Core inlet	°C	370	320	360–450	410	360	375	370
Core outlet	°C	430	480	600	530	550	525	500
Date of operation		1969	1974	1969	1970	1973		1973

As mentioned before, the cores of the reactors of the first generation were small and fueled with metal and their spectra were accordingly hard. The cores of the second generation are large and diluted and fueled with the mixed oxides, thus their spectra are comparatively soft. This affects the flux intensity in the resonance region of the cross sections involved, and the design of the second generation of fast breeders has to take these resonance phenomena into account in detail. In Figure 1 five spectra are plotted to exemplify this behavior: the effective σ_f of ^{239}Pu indicates the softness of the various spectra. In addition, the percentages of fission below 10 keV are compared in Table 4.

As these ceramic-fueled breeder reactors cannot rely on thermal fuel expansion as their main inherent stability feature, the Doppler coefficient must provide this stability. The fissionable isotopes give a positive contribution with temperature resonance broadening, whereas the fertile isotopes give a negative contribution, so that one must make sure of the sign and size of the Doppler coefficient of a given core composition (Table 5). Goertzel (54) was the first to calculate the Doppler coefficient, but he concentrated on the 100 keV region and neglected the region of stronger and more isolated resonances. Later, Nicholson (55) calculated this coefficient by a groupwise procedure covering the whole energy spectrum. Then the groups of Argonne, Karlsruhe, and GE (56–58) and others extended and refined the calculations.

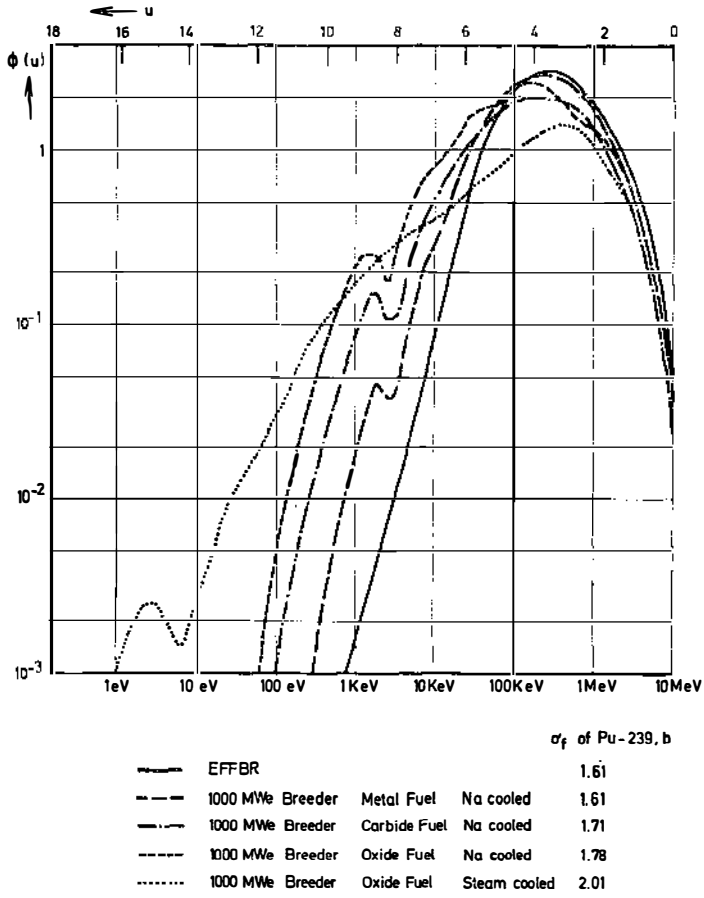

FIGURE 1. Neutron flux spectra of fast reactors.

Especially the treatment of overlap between resonances of the same sequence and of different sequences received much attention. It could be shown that the equation at b) (Table 6) is valid over the whole energy range; at high energies the overlap correction is rather accurate and equation b) is practically the same as a), while at low energies the correction term is less accurate, but negligibly small. The overlap of resonances of two different sequences can be ignored in the calculation of effective cross sections. Now the development of the theory is practically complete; survey papers on Doppler coefficient calculations were published by Nordheim (59) and by Nicholson & Fischer (60). Besides the standard method (Table 6) of

TABLE 4. Comparison of the relative fractions of fission for fast breeder reactors of the first and second generation

Neutron energy	EFFBR (first-generation fast breeder reactor)	Reference fast breeder reactor of the second generation
Below 9.1 keV	0.5%	9.6%
Below 40.7 keV	6.3%	25.2%
Below 67.0 keV	11.8%	35.5%

calculating effective cross sections, purely numerical methods were developed, which require high-speed digital computers.

For large ceramic reactors the Doppler coefficient is approximately proportional to $1/T$. Typical values for the so-called Doppler constant $T\delta k/\delta T$ (T temperature in °K, k criticality factor) for typical power reactor designs are

300 MW*e* Na-cooled prototype reactor: −0.0055 [Na−2 (61)]
1000 MW*e* steam-cooled reactor: −0.016 [D−1 (42)]

The first measurements of the Doppler coefficient were carried out in a facility simulating the hard spectrum of EBR-I (Kato & Butler 62) using cyclic heating of their samples. Baker & Jacques oscillated a hot sample versus a cold one (63). In the meantime quite a number of experiments have been

TABLE 5. Contributions to the Doppler coefficient

	Fertile isotope (^{238}U and ^{240}Pu)	Fissile isotope (^{235}U or ^{239}Pu)	Total
Changes in self-shielded cross sections	$\delta\tilde{\Sigma}_\gamma$	$\delta\tilde{\Sigma}_f$, $\delta\tilde{\Sigma}_\gamma$	
Contributions to Doppler coefficients			
Positive	—	$\nu\delta\tilde{\Sigma}_f\phi\int\chi\phi^+dE$	
Negative	$-\phi^+\delta\tilde{\Sigma}_\gamma\phi$	$-\phi^+(\delta\tilde{\Sigma}_f+\delta\tilde{\Sigma}_\gamma)\phi$	
Doppler coefficient at 900°C (17)[a]			
EFFBR (APDA, 1961)	− 2.0	+0.4	− 1.6
Large fast oxide breeder (GE, 1961)	−15.1	+5.1	−10.0

[a] In units of 10^{-6} $\delta k/k$.

$\delta\tilde{\Sigma}_x$ = Doppler change in the macroscopic self-shielded reaction cross section of type x ($x=f$: fission, $x=\gamma$: radiative capture)

ϕ, ϕ^+ = neutron flux and adjoint distribution

χ = fission spectrum

TABLE 6. Evaluation of self-shielded cross sections

$$\tilde{\Sigma}_x = \frac{\int \Sigma_x(E)\phi(E)dE}{\int \phi(E)dE} = \frac{\left\langle \frac{\Sigma_x}{\Sigma_t} \right\rangle}{\left\langle \frac{1}{\Sigma_t} \right\rangle} \qquad (NR \text{ approximation})$$

Σ = macroscopic cross section — x = type of reaction considered
t = total reaction — $\phi(E)$ = neutron flux at energy E
$\langle\ \rangle$ = average over resonances

a) Continuum region (small fluctuations):

Expansion with the parameter $\dfrac{\Sigma_t(E) - \langle\Sigma_t\rangle}{\langle\Sigma_t\rangle}$

leads to $\tilde{\Sigma}_x = \langle\Sigma_x\rangle - \dfrac{\langle\Sigma_x(\Sigma_t - \langle\Sigma_t\rangle)\rangle}{\langle\Sigma_t\rangle}$

$$\delta\tilde{\Sigma}_x = -\frac{\delta\langle\Sigma_x\Sigma_t\rangle}{\langle\Sigma_t\rangle}$$

b) Resonance region (nearly isolated resonances):

$$\left\langle \frac{\Sigma_x}{\Sigma_t} \right\rangle = \underbrace{\sum_k \frac{\Gamma_{xk}}{\Delta E}\int_0^\infty \frac{\Psi_k}{\beta_k + \Psi_k}\,dx_k}_{k\text{th isolated resonance}} - \underbrace{\frac{\langle\Sigma_x\rangle\langle\Sigma_c\rangle}{\sqrt{2\pi}\,\Sigma_p}\,F\left\langle \frac{\Delta}{\langle S\rangle} \right\rangle}_{\text{overlap correction}}$$

S = spacing of resonances — Δ = Doppler width
Γ = natural resonance width — β = reduced potential scattering cross section
ψ = ψ function = Maxwellian averaged Breit-Wigner cross section — Σ_p = potential cross section

c) *Overlap of resonances of two different sequences 1 and 2*

Expansion with the parameter $\dfrac{\Sigma_c^{(1)}\Sigma_c^{(2)}}{(\Sigma_p + \Sigma_c^{(1)})(\Sigma_p + \Sigma_c^{(2)})}$

leads in good approximation to $\tilde{\Sigma}_x^{(1)} \sim \dfrac{\left\langle \frac{\Sigma_x^{(1)}}{\Sigma_p + \Sigma_c^{(1)}} \right\rangle}{\left\langle \frac{1}{\Sigma_p + \Sigma_c^{(1)}} \right\rangle}$

performed with gradually increasing accuracy (64–67). For that it was necessary to relate the results of the measurements to reactor theory. This was first done by Storrer (68) and later by E. A. Fischer (69). Some typical results are shown in Table 7. For ^{238}U in Na-cooled assemblies the most recent analysis of an experiment in ZPR-6,5 with ENDF/B data gave calculated values that are about 25% too low in magnitude (66). Similar re-

TABLE 7. Typical results of Doppler experiments

Isotope	Reactor	Temperature range (°K)	$10^{-6}\ \delta k/k$ per kg fuel material: Measured	Expansion correction	Corrected	Calculated	Main core constituents (fuel/coolant)	References
^{238}U	ZPR-3, 43	300–800	− 4.6		− 4.6	− 5.1	UC/Na	64
	ZPR-3, 43A	300–800	− 7.9		− 7.9	−11.4	UC/Na+C	
^{239}Pu	ZPR-3, 45A	500–1000	− 4.9	+6.0	+ 1.1	+22.3	PuC-UC/Na	65
	ZPR-3, 45		− 2.5	+7.2	+ 4.7	+57.4	PuC-UC/Na+C	
^{238}U	ZPR-6, 5	300–1100	− 6.3		− 6.3	− 4.9[a]	UC/Na	66
^{238}U	SNEAK-3A-2	300–800	−16.9		−16.9	−17.0	UO_2/CH_2	67
^{239}Pu (with 8% ^{240}Pu)	SNEAK-3B-2		− 9.3	+1.5	− 7.8	− 6.8	PuO_2-UO_2/CH_2	68
^{238}U	ZPR-9, 13	300–1100	−44.6		−44.6	−59.0[a]	UC/Na+CH_2	218
^{235}U	ZPR-9, 13	300–500	+ 5.4		+ 5.4	+ 9.8[a]		
PuO_2-UO_2[b]	ZEBRA-5H	440	− 0.086		− 0.086	− 0.062	PuO-UO_2/Na	70

[a] ENDF/B data.

[b] $10^{-6}\ \delta k/k$ per °K and per kg mixed oxide fuel.

sults were obtained in a recent analysis of the ZEBRA Doppler loop measurements (70). The picture is different for assemblies containing hydrogen, where the prediction of the magnitude of the effect is either correct or too large (SNEAK 3A-2, ZPR-9,13). Therefore, the discrepancies may be due to errors in the calculated spectra. The measured effect in ^{239}Pu was much more negative than predicted in the Argonne experiments. Only in recent SNEAK experiments (in the spectrum of a steam-cooled reactor) could it be shown that fair agreement (to about 25%) can be reached for ^{239}Pu, if

a) samples with a scattering diluent (scattering cross section per atom of $^{239}Pu \approx 100$ b) are used to reduce the expansion effect, and

b) resonance parameters compatible with Gwin's high α = capture to fission ratio of ^{239}Pu are used between 0.1 and 10 keV (cf Figure 2).

A completely different approach for measuring the Doppler coefficient is to use power excursions of a properly designed fast test reactor. The GODIVA assembly of Los Alamos (71) and its experiments for determining the metal fuel expansion coefficient influenced the conception of this approach. The groups of Karlsruhe and GE independently developed this plan and later combined their resources to build up the SEFOR project (20). SEFOR is a reactor with a 500 liter core, UO_2/PuO_2 rods, and 20 MW*t* output. The rods are 1 inch thick in order to accommodate power output and temperature profile. Control is effected by a movable Ni reflector in order to have a clean core geometry. A fast-reactor excursion device allows for the rapid expulsion of a central absorber and thereby the introduction of reactivity ramp rates up to 200$/sec (1$ is the reactivity where the reactor becomes prompt critical) with various reactivity values (72, 73).

There are four basic schemes for measuring the Doppler coefficient:

1. By adjusting power output with primary and secondary cooling flow rates in a static run, the fuel, outlet, and inlet temperatures can each be kept constant and by that means the various contributions to the power coefficient can be roughly measured (74).

2. Ordinary oscillator tests will be executed. In addition, by adjusting power output with primary and secondary cooling flow rates in an oscillatory mode the fuel, outlet, and inlet temperatures can each be kept constant and by that means the various contributions to the power coefficient can be more accurately measured (75).

3. Subprompt critical reactivity steps will be introduced and the increase of flux after the prompt step, due to delayed neutrons, will be balanced against the decrease due to the negative power coefficient (76).

4. Superprompt critical excursions will be initiated by the introduction of reactivity ramps and the height and size of the flux peak will be measured in order to determine the Doppler coefficient and the effective ramp rate (77).

The SEFOR became critical in May 1969 and after initial zero power and startup tests the power experiments began in 1970. The plan for the sequence of experiments has been described in detail (78). Excursion tests to measure the Doppler coefficient were also pursued on VIPER in the UK (79, 80).

The next big challenge to fast-reactor physics after the Doppler coefficient was the understanding and the calculation of the Na void coefficient. Both the theoretical and the experimental treatment turned out to be difficult, as the effect is governed by differences of major effects. Removal of Na from a fast-reactor core affects the reactivity in three ways:

1. No more neutrons captured in Na (small positive effect).

2. Hardening of the spectrum; because of threshold fission in ^{238}U and because η increases with energy this is a positive effect in low-leakage reactors.

3. Increase of leakage (negative effect, dominates near core boundaries).

The Na void coefficient is negative in breeders of the first generation. It was first pointed out by Nims & Zweifel (21) in 1959 that the void effect might be positive in large ceramic reactors. The Na void coefficient, as well as the multiplication factor k, is mostly calculated in diffusion theory by the multigroup method, where the range of energies of the neutrons present in the reactor is divided into a suitable number of intervals, or energy groups. Accurate calculations of the Na void coefficient must be done in two dimensions, mostly as successive k calculations. To save computer time, a group condensation (from usually 26 groups to 4 to 6 groups) is often carried out first, with different weighting spectra in different parts of the reactor. Less accurate calculations can be done in one dimension or with perturbation theory for more general orientations. Therefore, no basic difficulty as to the

TABLE 8. Influence of the group cross sections

Comparison calculations of the sodium coefficient (219)

$\%\delta k/k$ for 50% Na removal (spectral and capture component)

	$^{238}U/^{239}Pu = 9$, no ^{240}Pu or fission products			$^{238}U/^{239}Pu = 9$, ^{240}Pu and fission products		
	Spectral	Capture	Total	Spectral	Capture	Total
ANL 300°	2.02	0.29	2.31	3.16	0.22	3.38
France 900°	2.08	0.28	2.36	3.20	0.15	3.35
GE	1.37	0.19	1.56	2.67	0.15	2.82
UK 300°	1.34	0.27	1.61	3.20	0.20	3.40
Karls-ruhe 900°	—	—	—	3.37	0.27	3.64

method of calculation exists. The difficulty is much more with the sensitivity of the results with respect to the multigroup cross-section data. This is so because the moderation effect, which dominates at least in the center of the core, depends essentially on $d\phi^+/dE$ (ϕ^+ adjoint flux). This sensitivity can be recognized from Table 8.

The principal tool for investigating the Na void effect experimentally is the fast critical facility. A survey of existing facilities is given in Table 9. Measurements have been made at ZPR-3, ZPR-6, ZEBRA, SNEAK, and elsewhere. A particular difficulty in interpreting the measured results is the heterogeneity effects due to the fine structure (platelets or rodlets). During the first generation of fast breeder reactors, these effects could be ignored because of the hardness of the spectrum, but the softer spectrum of the second-generation reactors requires a better evaluation of them, particularly for the Na void effect. This combined space-energy dependence for isotopes with resonances present in platelets including the interactions between isotopes requires detailed and cumbersome calculational approaches (81–83). Table 10 gives typical experimental and theoretical results (84–86).

As already mentioned, the more complex physics of second-generation fast breeders requires a much improved calculational technique. Since the spectrum of the first-generation breeders was hard enough not to cover the resonance area, it was adequate simply to superpose the cross-section contributions of the various isotopes present in the core. Therefore it was possible to establish universal sets of group constants. The mode of averaging these universal group constants within one energy group was fairly unsophisticated and simple (87). The most widely used such set was the YOM set (88). But with improved calculational techniques and the investigation of the Doppler coefficient it became clear that the energy self-shielding must be taken into

TABLE 9. Fast critical assemblies

	Location	Year first critical	Short description	Fissile material	Typical core size, liters (for average reflector thickness)
ZPR-3	Argonne, Idaho	1955	Horizontal, split-table machine	^{235}U, ^{239}Pu (600 kg)	600
ECEL	Atomics International, California	1960	Horizontal, split-table; thermal driver	^{235}U, 25 kg of ^{233}U were used in some assemblies	100 (test zone)
VERA	Aldermaston, UK	1961	Vertical, split-table	^{235}U, ^{239}Pu (40 kg)	400
BFS	Obninsk, USSR	1961	Vertical, fixed	^{235}U	1800
ZEBRA	Winfrith, UK	1962	Vertical, fixed	^{235}U, ^{239}Pu (400 kg)	3000
ZPR-6	Argonne, Illinois	1963	Horizontal, split-table	^{235}U	3000
ZPR-9	Argonne, Illinois	1964	Horizontal, split-table	^{235}U	3000
FRO	Studsvik, Sweden	1964	Vertical, split-table	^{235}U	65
MASURCA	Cadarache, France	1966	Vertical, fixed	^{235}U, ^{239}Pu (200 kg)	3000
SNEAK	Karlsruhe, F.R. of Germany	1966	Vertical, fixed	^{235}U, ^{239}Pu (200 kg)	3000
FCA	Tokai-Mura, Japan	1967	Horizontal, split-table	^{235}U, ^{239}Pu planned	3000
ZPPR	Argonne, Idaho	1968	Horizontal, split-table	^{235}U, about 3000 kg of ^{239}Pu planned	3000
STEK	Petten, the Netherlands	1969	Vertical, fixed, thermal driver	^{239}U	250

account. This implies terms of the nature $\psi/(\beta+\psi)$ with ψ being the Maxwellian averaged Breit-Wigner term for a resonance cross section and β being essentially the potential scattering cross section, which is composed of the contributions of all isotopes present in the reactor core. As this is a nonlinear term, it is no longer possible to establish universal sets of group constants. In addition, with improved accuracy of the calculational methods, it is necessary to take into account the composition-dependent weighting spectrum within each (coarse) group. For both reasons, it is necessary to have first a program to prepare group constants for each particular reactor composition in question as an input for an extended multigroup calculation, e.g. the MC^2 program of Argonne (89), the Galaxy program of UKAEA (90), and the MIGROS program of Karlsruhe (91). Because of the term $\psi/(\beta+\psi)$ these programs necessarily refer to the temperatures of the various isotopes. Preparing two different runs for two different temperatures permits calculation of the various temperature coefficients. Very often a zero-dimensional or one-dimensional many-group calculation is run first (e.g. 60-group or even more) and the resulting energy spectrum is used to prepare for each individual core or blanket composition and core or blanket section a condensed individual set of (coarse) group constants, which are finally used in a multidimensional calculation.

An example is the 25-group-constant set of Argonne for calculating certain criticals in ZPR-3 and ZPR-9 (66). Somewhat older and more widely

TABLE 10. Sodium void effect, 10^{-5} $\delta k/k/kg$

		Experiment	Perturbation calculations				References
			Abs.	Mod.	Leak.	Total	
ZPR-6, Ass. 3:	950 liter pancake core; enriched U, carbide						
Central region, 15.2 cm high 18.7 cm diam		0	−3.22		− 0.98	− 4.20	84
Total core		− 6.30	−0.27		− 5.80	− 6.07	
ZPR-6, Ass. 4Z:	Zoned core, central region; 2600 liter carbide core						
Central region, 10.1 cm high 20.4 cm diam		+ 2.3[a] + 2.0[b]				+ 4.0	85
Region along axis, full core height 20.4 cm diam		−10.0[a] −17.3[b]				+ 4.78	
ZPR-3, Ass. 48:	Pu-carbide core						
Central region, 10.16 cm high 14.3 cm diam		+ 8.4± 0.8	3.43	4.52	− 1.68	+ 6.27	86
Axial edge		−21.9± 0.3	0.77	3.41	−30.7	−26.5	
SNEAK-2C:	PuO_2/UO_2 core						
Central region, 17.4 cm high 12.3 cm diam		+ 9.0				+ 8.7	
Region along axis, full core height 12.3 cm diam		+ 0.40				− 1.10	

[a] Na next to ^{238}U.
[b] Na next to C.

known is the Russian ABN 26-group set. It covers the energy range from 10 MeV to thermal. Most of the energy groups have a lethargy width $\Delta u = 0.77$. Various energy self-shieldings due to various potential scattering cross sections are listed and interpolation is possible (92). The Karlsruhe group has established group-constant sets for some of their reference designs (93); General Electric starts mostly with their 60-group set and condenses from there to the considered special cases (94). The case of the scattering resonances requires special treatment. Argonne had developed as early as 1961 a several hundred-group set in the spatial ground mode approximation and derives from that properly condensed transport group constants (95). Some of the more modern codes for preparing group constants contain more modern versions of that code (96).

The extremely refined calculational technique is of course very sensitive to the microscopic data input, while a tremendous input of microscopic cross-section data is needed to run the above-described sophisticated calculations. In order to get these microscopic input data the European American

Nuclear Data Committee EANDC compiled the various requests (97) and for example the Cross Section Evaluation Working Group at Brookhaven has compiled an Evaluated Nuclear Data File for Reactor Applications (ENDF/B) (98, 99). The Karlsruhe group has also been very active in that field (100, 101). A similar European activity is concentrated at Saclay (102). The International Atomic Energy Agency IAEA has been making evaluations and coordinating on a worldwide basis for some time.

In this survey paper only the most important recent advances in the area of microscopic cross sections can be reported. The most striking was the Schomberg measurements of the capture to fission ratio α of ^{239}Pu (103). The "^{239}Pu-α problem" was discovered by Schomberg et al at the Karlsruhe Conference in 1967. They reported measured values of α between 0.1 and 10 10 keV, more than twice as large as those based mainly on KAPL measurements in 1957, accepted until then. However, the experimental method used by Schomberg at the Harwell linac was new and not yet developed to good accuracy. Since then, several further measurements have been performed in different countries. The important ones are shown in Figure 2. Gwin et al measured α at the Rensselaer linear accelerator (104). As they used a detector that had been tested in earlier experiments and as the uncertainty of their data is rather small (15%), these data are considered to be the most reliable at present. They are about halfway between the old KAPL data and the 1967 Schomberg data. They are also supported by evaluations of α from the total and the fission cross section, as carried out by Pitterle (105) and by Ribon (106). These evaluations are also shown in Figure 2. Schomberg et al (107)

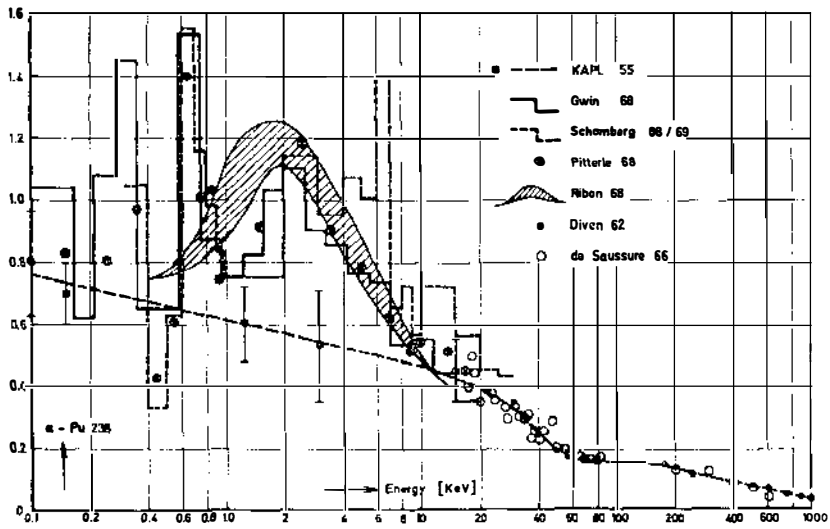

FIGURE 2. α-Pu 239.

repeated their measurements in 1968 under improved experimental conditions; the results are lower than in their earlier experiments and agree well with Gwin's below 4 keV, but are higher between 4 and 30 keV. Further measurements were carried out by Ryabov et al (108) at Dubna. Their results are, in part, even below the old KAPL values. They are not shown in Figure 2, because the authors could identify some inconsistencies; therefore, it is planned to repeat the experiments. It is now well established that Pu-α is well above the old KAPL data and below the 1967 Schomberg data and should be close to the Gwin data. This conclusion is supported by integral experiments, which consist of establishing the reaction rate balance in soft-spectrum null-reactivity assemblies on ZPR-3 (66) and ZEBRA (109), and also by Doppler experiments with Pu samples carried out on SNEAK at Karlsruhe (69). However, the uncertainty in the 6 keV range between the Gwin data and the 1968 Schomberg data remains.

The Pu-α problem is also important in nuclear physics. All the recent measurements show strong fluctuations of α as a function of energy, which have recently been explained as due to intermediate subthreshold fission. This phenomenon can be explained by a theoretical model due to Strutinsky (110), which is a modification of the liquid-drop model. The important feature of the model is a second potential minimum at some strong deformation, in addition to the main dip at the ground-state deformation. The levels in this second dip are much wider spaced than in the main dip, and correspond to the minima of α (E). A more detailed description may be found in (111).

Another important datum is the capture cross section of ^{238}U. Figure 3 shows the capture cross section of ^{238}U as recommended by J. J. Schmidt in

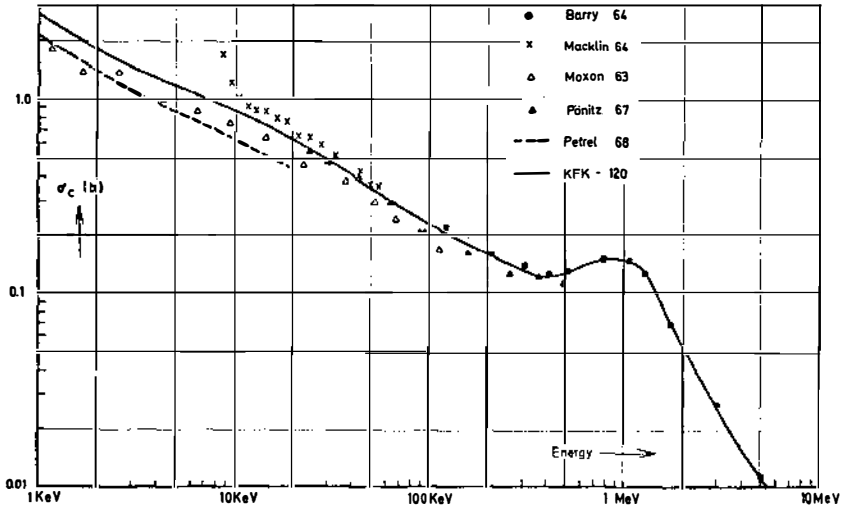

FIGURE 3. Capture cross section of U 238.

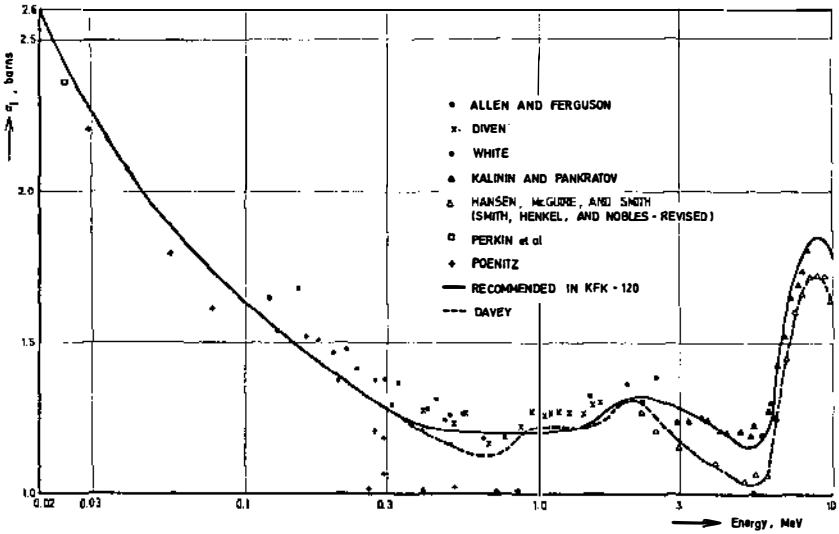

FIGURE 4. Fission cross section of U 235.

1966 (100). The measurements shown in Figure 3 show rather large deviations from each other. More recent measurements of Glass et al (112) obtained from the Petrel nuclear explosion lead to the dashed line in Figure 3. The Poenitz data (113), which are normalized to an absolute measurement at 30 keV, also tend to be below the Schmidt data. Although there are even today large deviations between the different data, it seems fairly certain that σ_c is lower than the Schmidt curve in the keV range. This conclusion is supported by comparison with integral data (114).

Major changes also occurred for ^{240}Pu. Since the ABN cross-section set was prepared (92), knowledge of resonance parameters of ^{240}Pu was improved mainly by measurements of the Geel group (115, 116). Therefore it is not surprising that recent evaluations by Yiftah et al (117) and by Pitterle (118) suggested that the old values σ_f and σ_c should be drastically revised. The new capture cross section is about a factor of 2 lower than the ABN values. The major changes of σ_f are due to subthreshold fission below 200 keV. It is interesting that calculations with the Pitterle data agree much better than ABN data with integral material worth experiments as carried out by Oosterkamp (111).

Attention must be given also to the fission cross section of ^{235}U as this is often used as a normalization standard. Figure 4 reviews the present situation (119, 120). Notice the clear discrepancy between the data of Poenitz (122) and all others.

As to ^{239}Pu, there are three precision measurements of the ^{239}Pu to ^{235}U σ_f ratio above 20 keV, by Allen & Ferguson, by White et al (123), and re-

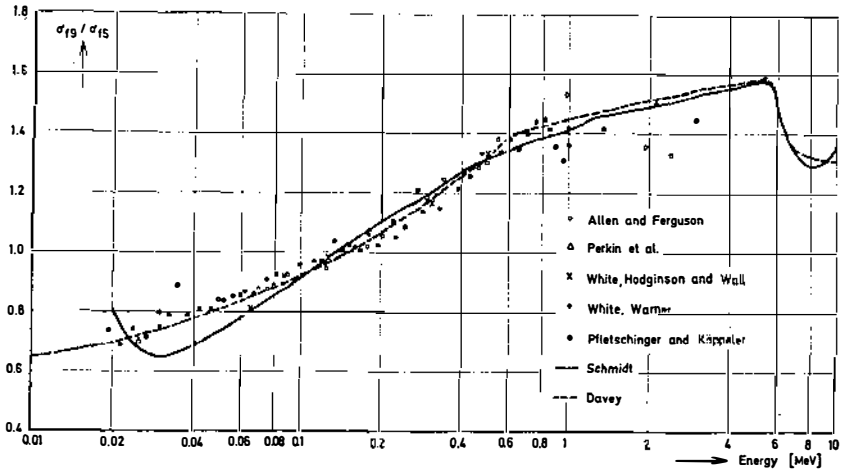

FIGURE 5. Ratio of Pu 239 to U 235 fission cross section.

cently by Pfletschinger & Kaeppeler at Karlsruhe (124). Figure 5 shows the data together with the evaluations by Davey (121) and Schmidt (101).

During fast-reactor physics work for the first generation of fast breeders, virtually no attention was given to fission-product cross sections. But with the softer spectrum and considerably higher burnups of the second generation breeders this becomes gradually more important. There are three roads to improved information in this field. The first road is differential cross-section measurement. After an early compilation by Garrison & Roos (125) there is a more recent set of data by Benzi & Bartolani (126). The second road is the selection of nonradioactive and the simulation of radioactive fission-product isotopes and subsequent measurement in a fast critical facility (127). The third road is the direct measurement of the fission-product poisoning in a critical facility specifically designed for the use of highly radioactive oscillator samples containing these fission products. In the Dutch research center Petten such a facility, called STEK, has been built as a part of the German-Dutch-Belgian-Luxembourg fast-reactor project (128); it first became critical at the end of 1969. Directly applicable and precise results are expected soon.

From the above explanations it is clear that there are three subsequent regions of theoretical effort: the evaluation of microscopic data, the preparation of specific sets of group constants for specific cases, and the multigroup multidimensional calculation together with a code for evaluating reaction rates or other reactor data. Having reviewed each of these three regions in reverse order, one inevitably asks: how large are the various changes using different sets of data and how good is the agreement between reactor theory and reactor experiment? To indicate this, an example taken from the work of

TABLE 11. Comparison of measured and predicted integral data

	k_{eff}				σ_{f8}/σ_{f5}				Weighting spectrum
	Exp	KFK	PMB	MOXTOT	Exp	KFK	PMB	MOXTOT	
ZPR-3, 48	1.000	0.979	0.989	0.990	0.0307	0.0300	0.0309	—	NAP
ZEBRA-6A	1.000	0.970	0.976	0.976	0.0364	0.0347	0.0357	—	NAP
SNEAK-3A-1	1.000	0.990	0.981	1.014	0.0336	0.0301	—	—	SNEAK
SNEAK-3A-2	1.000	0.983	0.977	1.005	0.0313	0.0294	0.0295	—	SNEAK
SNEAK-3B-2	1.000	0.978	0.979	0.993	0.0289	0.0233	—	—	SNEAK
	σ_{c8}/σ_{f5}				σ_{f9}/σ_{f5}				Weighting spectrum
	Exp	KFK	PMB	MOXTOT	Exp	KFK	PMB	MOXTOT	
ZPR-3, 48	0.138	0.146	0.144	—	0.976	0.908	0.941	—	NAP
ZEBRA-6A	—	—	—	—	0.961	0.899	0.928	—	NAP
SNEAK-3A-1	0.142	0.143	—	—	1.03	0.96	—	—	SNEAK
SNEAK-3A-2	0.130	0.136	0.136	—	1.01	0.95	0.99	—	SNEAK
SNEAK-3B-2	—	—	—	—	0.94	0.83	—	—	SNEAK

the Karlsruhe fast breeder project appears in Table 11. Three spectral indices and k_{eff} have been calculated for one ZPR, one ZEBRA, and three SNEAK criticals. The experimental values are given together with the results of three theoretical calculations. KFK indicates a group-constant set that has been prepared for certain reference studies (114), and PMB indicates an improvement of the microscopic input data by taking into account the low ^{235}U σ_f and the low ^{238}U σ_c data by Poenitz et al (see Figures 3 and 4) (129), whereas MOXTOT indicates use of new data (130), especially the high Pu-α Gwin data (104), the low data for ^{240}Pu (117, 118), and the MOXON data for σ_c of ^{238}U as reported in Figure 3 of this paper. NAP and SNEAK refer to different weighting spectra of the various group-constant sets, such as the ZPR-3 and ZEBRA critical mockup, a Na-cooled, and the SNEAK-3A, a steam-cooled reactor. One concludes that 1% accuracy for k_{eff} and 3% accuracy for the spectral indices are not yet really achieved goals.

More general evaluations have been made to assess the influence of uncertainties in microscopic data on reactor variables. To be mentioned here are the papers of Greebler (131) and more recently of Barre (132).

Further, the results of a worldwide intercomparison of calculating some integral quantities of the assembly ZPR-3, 48, typical of a large fast Pu ceramic-fueled core, are given in Table 12. The figures there are the ratio between predicted theoretical and actual experimental data (86, 133–139). In this worldwide intercomparison the uncertainty in k_{eff} is 2%, in the reaction rates 10%, in material worth 10%, in central Na worth $\pm$ 200%.

This consideration can perhaps be brought to an end best by stating that the prediction of k_{eff} is within 3–4% (critical mass: 15–20%), if a particular case is calculated and the group-constant set is chosen without care among the sets in use. If one instead chooses or prepares the group-constant set with

TABLE 12. Ratio between calculation and experiment for some integral measurements in ZPR-3, 48

	ANL 66	Karlsruhe 66	GE 67	APDA 67	Karlsruhe 69	GGA 69	AI 69	ANL 69	Cadarache 69
k_{eff}	1.024	0.989	0.997	0.992	0.987	—	1.024	0.987	1.006
Reaction rates									
σ_{f8}/σ_{f5}	1.02	0.96	1.01	0.93	0.91	0.96	0.93	0.98	1.005
σ_{f8}/σ_{f5}	1.03	1.00	1.00	0.97	0.94	0.96	0.97	0.96	1.02
σ_{c8}/σ_{f5}	0.92	0.95	1.00	0.93	0.94	1.07	0.90	—	—
Material worth									
^{239}Pu	1.06	1.02	1.01	1.02	0.96	1.02	0.95	1.00	0.95
^{238}U	0.86	0.87	0.92	1.00	0.91	1.24	0.86	1.03	
Na	0.70	2.00	0.40	1.00	2.00	0.25	2.4	−1.00	

care, but without special experimental assistance, the prediction of k_{eff} is within 1.5–2% (critical mass: 8–10%). If in addition to the latter case the results of a similar critical experiment are available, it should be possible (140) to predict k_{eff} within 0.5–1% (critical mass: >5%).

Finally, a remark should be made on the interconnection of extended reactor physics calculations and computer capabilities. The Na void calculations in particular and the calculation of large fast second-generation breeders in general require as of today three-dimensional calculations: in the case of the Na void effect for instance two space dimensions and one energy dimension. This just fits the calculational capability of today's computers, say IBM-360/65 (or better-360/91) or CDC-6600. Some years ago all reactor problems were treated only in two dimensions (one space, one energy dimension or one space, one time dimension). It is probable that, as the art develops, four dimensions can and must be handled and this requires the next generation of big computers. It should be realized how strong this interlink is (see Table 13).

THE FUEL ELEMENT

A burnup of ~50,000–100,000 MWd/ton is mandatory for the economy of fast breeder reactors and this was essentially the reason for going from the first to the second generation of fast breeders, leaving metal as a fuel behind and concentrating mainly on UO_2/PuO_2 fuel (16, 141). The main concern in former years was the swelling of the highly irradiated fuel due to fission products and in particular fission gases (9). But today the problem is very different as it is rather the cladding material and the associated irradiation damage that causes the main concern. Therefore the first point of this discussion will be the cladding material. A 100% burnup of all fissionable isotopes of the original fuel, which is desirable for an economic fuel cycle

TABLE 13. Fast-reactor calculations and computer capabilities

Generation	Year	Typical computer	Maximum number of dimensions for parameter studies	Maximum number of dimensions for single calculations
1	1954–1960	UNIVAC I and II IBM 650	1 (e.g. zero-dimensional multigroup calculations)	2 (one-dimensional multigroup diffusion calculations)
2	1960–1965	IBM 7090 UNIVAC 1107	2 (1-*D* diffusion calculations)	3 (1-*D* burnup calculations, 2-*D* diffusion calculations)
3	1965–1968 from 1968 on	CDC 6600 IBM 390/91 IBM 360/85 CDC 7600	3 (1-*D* burnup calculations, 2-*D* diffusion calculations)	4 (3-*D* diffusion calculations)

operation, requires fluences $\phi \cdot t$, which obey the following self-explaining relation:

$$\sigma_f \cdot \phi t = 1$$

According to the effective fast fission cross section as given in Figure 1, this leads independently of any other parameter to a fluence of roughly 5–7 $\cdot 10^{23}$ for 100% burnup of all original fissionable isotopes. In fast reactors the other cross sections, σ_s and $\sigma_{n,\alpha}$, which are relevant for radiation damage in the cladding material are now much more comparable in size to σ_f than is the case in thermal reactors. In thermal reactors the ratio of total reactions $(\sigma_s \cdot \phi t)/(\sigma_f \cdot \phi t)$ is lower by two orders of magnitude as compared with fast reactors! If $\sigma_f \cdot \phi t \sim 1$ is fulfilled in fast reactors, every single atom of a metal lattice has also been hit by a neutron roughly once during its lifetime and this explains why types of radiation damage that are unknown in thermal reactors come into the picture.

There are basically three types of radiation damage. The first is the well-known lattice displacement. Incident neutrons and their secondary effects cause displacements in the metallic lattice; this becomes increasingly severe with decreasing temperature and is therefore called *low-temperature embrittlement.* Above 400°C or so the annealing rate of this type of irradiation damage is large enough to repair the lattice and thereby to overcome the damage (142, 143).

The second type of damage is the formation of He bubbles at the grain boundaries by (n,α) reactions. To expedite the formation of significantly large He bubbles a certain mobility of the He atoms is required, which in turn is available at sufficiently high temperatures. A temperature range above 500°C seems to provide the needed mobility and this phenomenon is therefore called *high-temperature embrittlement* (144–147). It increases with

temperature and leads to a reduction of applicable strains (148–151). Many isotopes that appear as components of modern alloys have significant (n,α) cross sections now and therefore lead to large enough He formation rates at large enough fluences (152–154). A fluence of $\sim 10^{23}$ *nvt* is required for the presently envisaged 300 MW*e* class of fast-reactor prototypes; the corresponding fluence of a thermal-neutron reactor is lower by the factor of σ_f fast/σ_f thermal$\simeq$200 and therefore is only $\sim 10^{21}$ *nvt*. Remarkably enough, it is beyond a fluence of 10^{22} *nvt* referring to $\sigma_{n,\alpha}$ cross sections $\sim$1 mb that the high-temperature embrittlement becomes important! The impact of this phenomenon has therefore never been felt in the thermal-reactor domain.

The third type of irradiation damage is void formation by vacancy condensation (155, 156). During the last 2 or 3 years it has become obvious that the swelling rates of cladding materials beyond fluences of 10^{22} *nvt* were larger than could be explained by the above-mentioned He high-temperature embrittlement. Today it seems sufficiently certain that there is a kind of condensing mechanism of vacancies, which is governed by the equilibrium between rates of void formation and rates of void annealing together with the presence of condensation nuclei. It now seems that in particular the helium atoms of the above-mentioned (n,α) reactions act as such condensation nuclei. The additional vacancy condensation effect therefore seems to explain the higher swelling rates, which cannot be explained by (n,α) reactions. The amount of He formation is a function of the fluence alone and this is therefore the main variable, but the rate of void formation depends on flux *and* fluence and therefore introduces the flux as an additional variable. Similarly, as with the above considerations on the fluences, one can see that fast reactors must have a high flux.

The other variable, which besides burnup ($\sigma_f \phi t$) mainly governs the economy of a fast reactor, is the fuel rating b in MW*t*/kg fiss mat. as it is responsible for the interest of the inventory of fissionable material at a given power output. But b is directly proportional to $\phi\sigma_f$ without any other parameter in the equation. In both thermal and fast reactors, a value of $b \simeq 1$ MW*t*/kg fiss mat. is required for general reasons of economy (16, 141). Therefore we have

$$\frac{\phi_{\text{fast}}}{\phi_{\text{thermal}}} = \frac{\sigma_{f\ \text{thermal}}}{\sigma_{f\ \text{fast}}}$$

The fluxes have to be larger again by that factor of $\sim$200! So this vacancy-condensing phenomenon that depends on flux is typical for fast reactors and has not been observed in thermal reactors. The above-mentioned last two phenomena and their various interactions have not yet been fully understood. The main hindrance is the lack of sufficient experimental data. It has been mentioned in the introduction that the breeders of the first-generation EBR-II, DFR etc are being used as test reactors for the fuel of the second-generation breeders. This certainly is the case, but their neutron fluxes are

TABLE 14. Neutron flux of fast reactors

	Existing Reactors				Projected Prototypes			
	EFFBR Core A	EBR-II	DFR	RAPSODIE	RAPSODIE fortissimo	EFFBR oxide-core	PHENIX PFR	SNR
Reactor power MW*t*	200	42	60	22	40	430	530	730
Total-neutron flux [$\times 10^{15}$ n/cm^2 sec]	4.73	2.07	2.5	1.8	3.0	8.2	7.0	8.7
Neutron flux above 0.11 MeV [$\times 10^{15}$ n/cm^2 sec]	3.51	1.77	2.22	1.6		5.0	4.1	4.8

lower by a factor of ~ 4 ($\simeq 2 \cdot 10^{15}$ n/cm^{2}sec) as compared with the fluxes of the now envisaged 300 MW*e* fast breeder prototypes ($\simeq 8 \cdot 10^{15}$ n/cm^{2}sec). Therefore it takes $2\frac{1}{2}$ calendar years to achieve under practical and day-by-day operational conditions a fluence of 10^{23}, for example in the DFR in Scotland (see also Table 14). Large sets of canning material irradiations are under way and significantly more irradiation results are expected in 1971.

On the basis of these explanations, a number of results and features of high-fluence, high-flux canning materials for fast reactors will now be presented in a phenomenological fashion. Figure 6 presents the swelling $\Delta V/V$ of stainless steel at various fluences (157–162). Values as high as 10% have been observed, but much lower values at the same fluence have been observed too. Stainless steel is still the choice for Na-cooled fast reactors in the near future (163). Steam-cooled reactors, on the other hand, required a strong Ni component for reasons of dry-stream corrosion resistance, either in the form of an Incoloy 800 type of steel or in the form of a Ni-base alloy on the Inconel 650 type (164, 165). But the strong (n,α) reaction of Ni usually leads to much stronger swelling rates as compared with stainless steel and this has partly been the reason for dropping steam (166). The swelling of stainless steel now has two implications, the absolute value and the flux and temperature dependence of the swelling. The absolute value of the swelling in absence of flux or/and temperature gradients can be simply accommodated by straightforward core design measures. But the flux and temperature gradients in the core give rise to fairly strong bowing effects and therefore more complex design difficulties. To assess and compare these various design difficulties some workers have tried to interpolate on a pragmatic basis the wide-spreading experimental results by a reasonable working formula. As there is no full theoretical understanding of the phenomena involved, quite a variety of mathematical expressions can be assumed. The

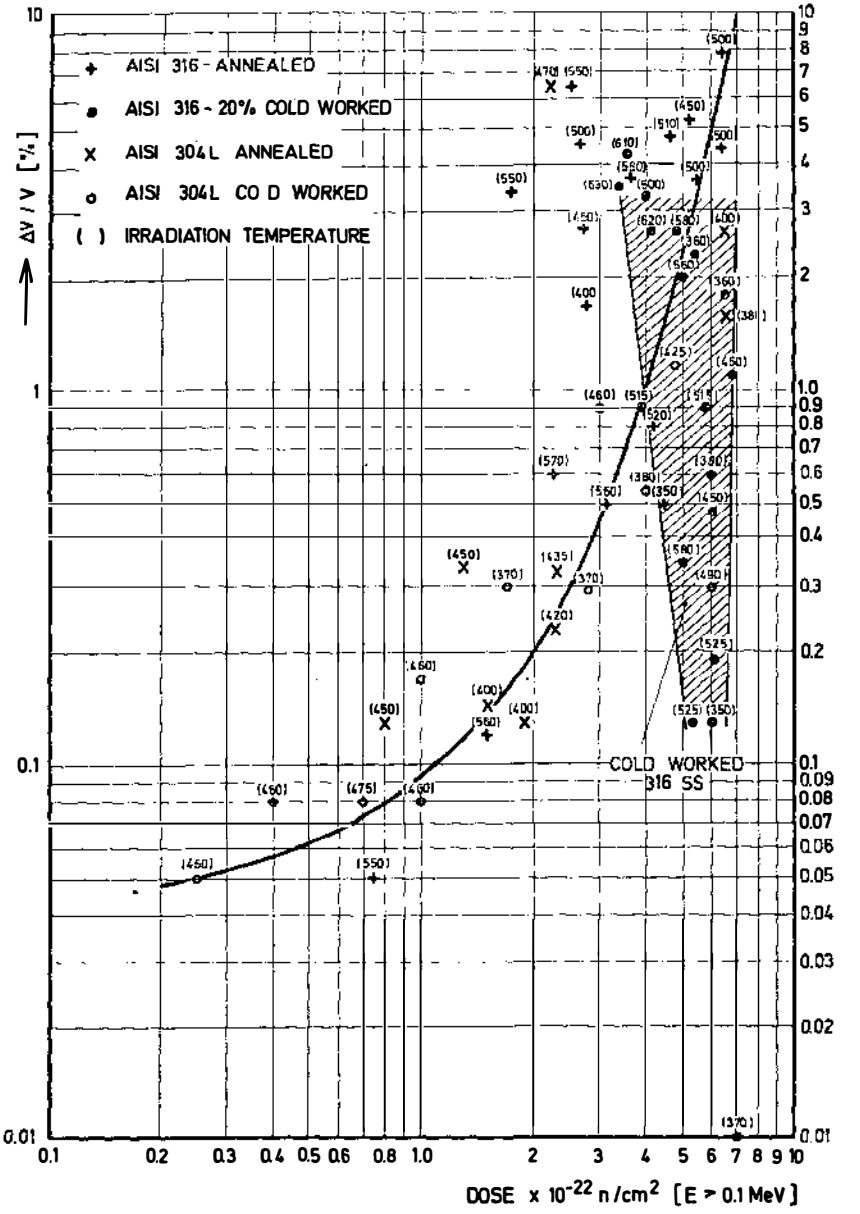

FIGURE 6. Swelling of stainless steel.

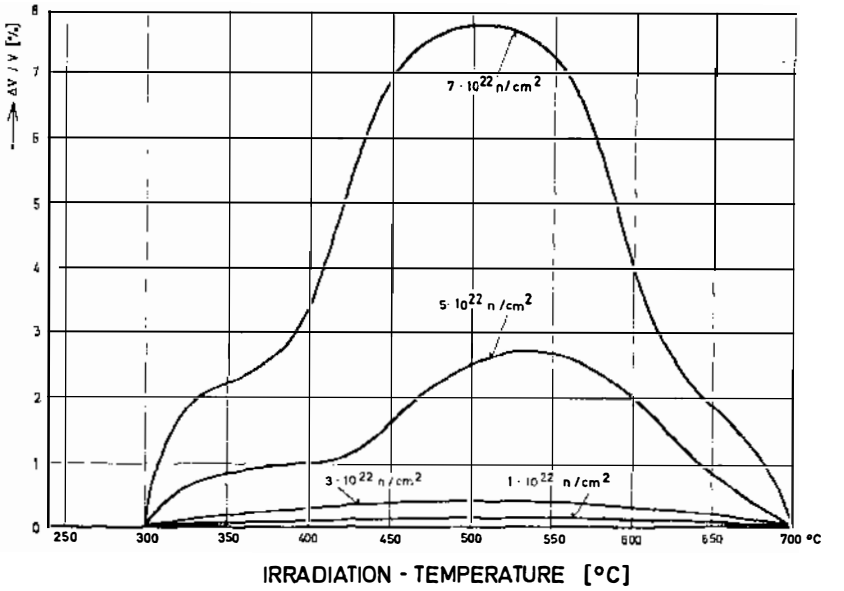

FIGURE 7. Predicted effect of irradiation temperature and fluence on void volume in type 304 stainless steel.

German group for instance has adopted the following formula:

$$\frac{\Delta V}{V}(\%) = 8.5\left(\frac{\phi \cdot t}{10^{23}}\right)^{1.6} \exp\left(-\frac{(T - 490)^2}{10{,}000}\right)$$

T in °C, ϕt = fast fluence ($E \geq 0.1$ MeV)

Figure 7 shows the $\Delta V/V$ values according to this formula (167). Another example is the expression of Claudson & Barker (168):

$$\frac{\Delta V}{V}(\%) = 5.0 \cdot 10^{-36}(\phi t)^{1.6} \exp\left(-\frac{6800}{RT}\right) - 1.87 \cdot 10^{4} \exp\left(-\frac{27{,}000}{RT}\right)$$

These values are given for four temperatures in Figure 8. The existence of a mathematical expression should, however, mislead nobody about the large errors and uncertainties involved.

The other more general feature of these fast-neutron irradiation damages is a considerable reduction of the applicable creep-rupture strengths. Figures 9a and 10a show typical results for the applicable tangential stress

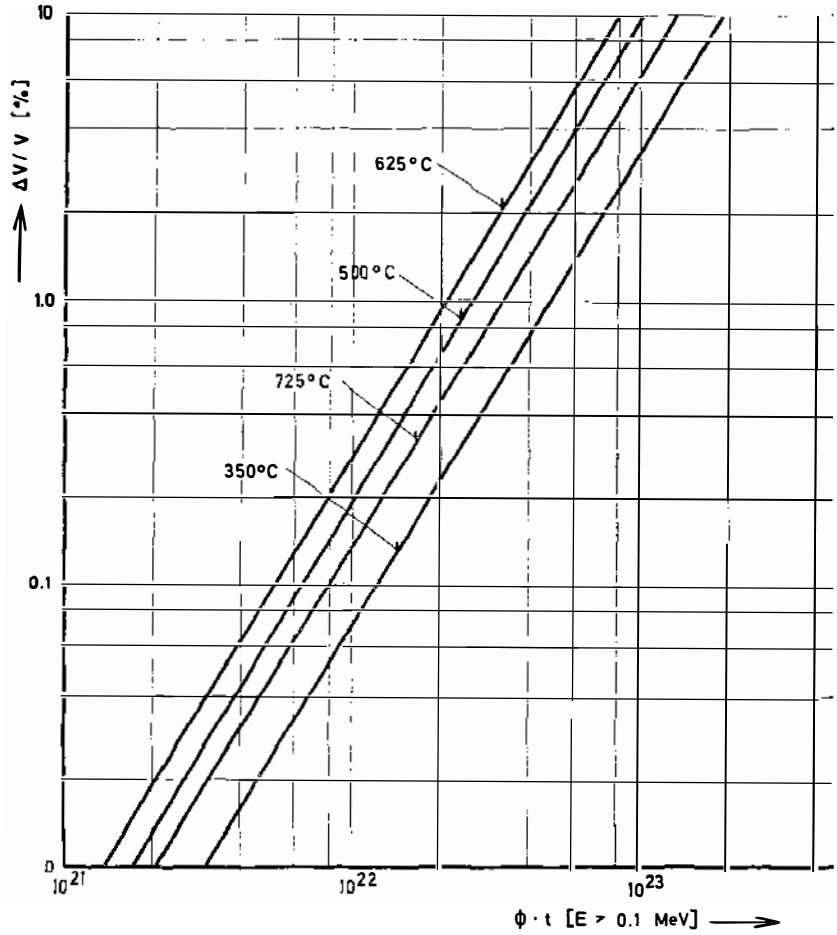

FIGURE 8. Swelling of stainless steel (AISI 304 and 316).

leading to failure (169, 170). In this example an irradiation of $\simeq 7 \cdot 10^{21}$ n/cm² leads to a reduction of about 40–50%. Along with the reduction of creep-rupture strength goes a general reduction of ductility as the high-temperature embrittlement comes into the picture. Figures 9b and 10b give an insight into that effect (171). For present fuel pin and core designs the fast-reactor designers have to assume values of the creep strain as low as 0.5–1%. To complicate things further, the influence of radiation damage on the ductility depends on the applied stress configurations. Multiaxial configurations in the presence of irradiations lead to reductions of the ductility that are more severe than under unirradiated conditions.

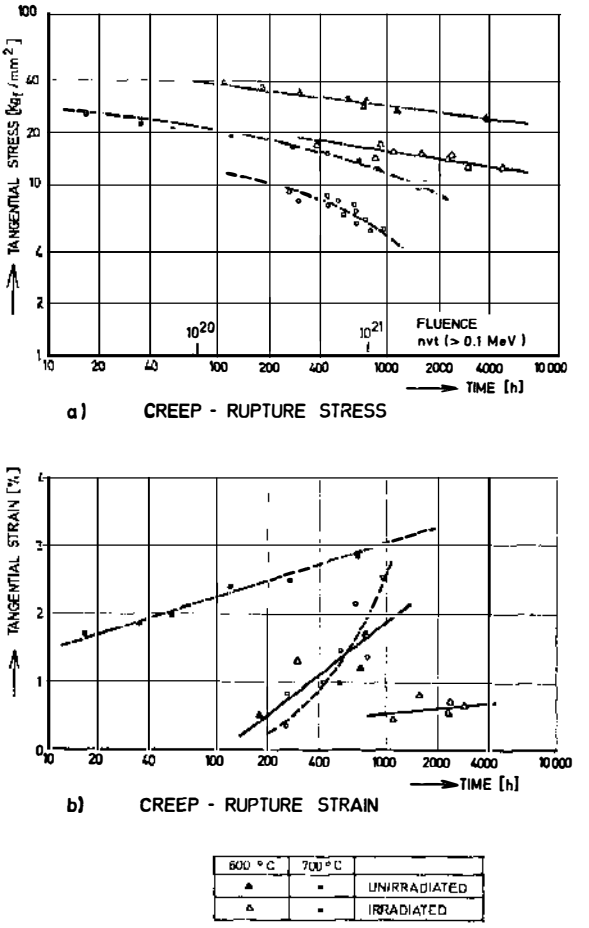

FIGURE 9. Creep-rupture strength of stainless steel tubes (16 Cr 13 Ni).

As mentioned before, the most widely accepted choice for Na-cooled reactors is stainless steel, as the corrosion of Na can be controlled if the oxygen content of Na is sufficiently low ($\lesssim$ 50 ppm) and the irradiation damage seems manageable (172, 173). The other important limiting factor is the maximum cladding temperature. Most designers have accepted 700°C as the maximum hot spot, midwall cladding temperature. Other solutions are sought in advanced designs because such a temperature limitation severely limits the thermohydraulic core performances. It seems possible that vanadium-base alloys can overcome these limitations (174).

The question of cladding materials exposed to fast-neutron irradiation, stresses, and high temperatures is very broad but a more detailed review is

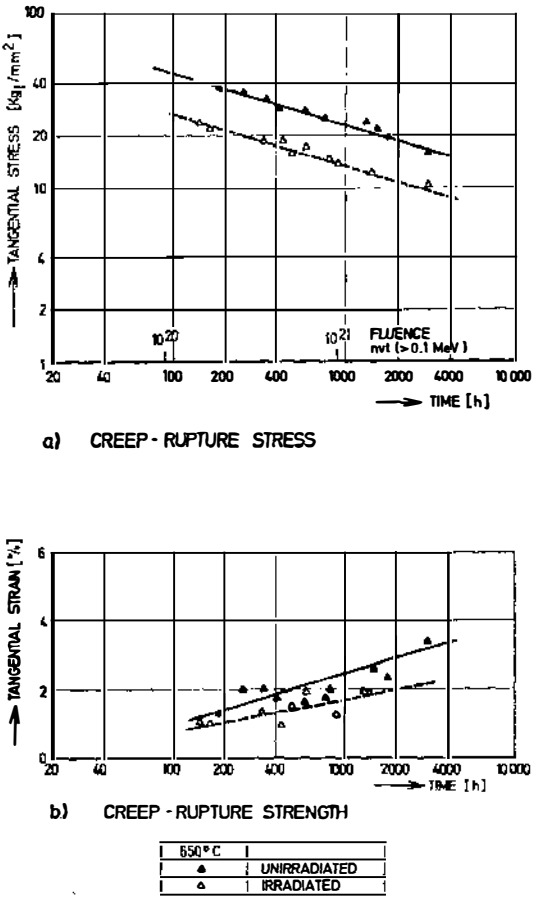

FIGURE 10. Creep-structure strength of inconel 625 tubes.

impossible here. Therefore reference is being made to more specific review articles and proceedings of special conferences (163, 175, 176). The cladding material is used for the design of the fuel pin. A remarkable feature of fast-reactor development is the worldwide acceptance of and agreement on the specifications of fuel pins for the envisaged 300 MW*e* prototype class. These specifications follow the concept of a mixed oxide fuel with low density. From numerous irradiation experiments it is well established that shortly after the beginning of irradiations a central hole forms in the axis of the fuel and the fuel pellets occupy an annular configuration within the cladding cylinder (177) (see Figure 11). After sufficiently long irradiation times, the final configuration depends almost not at all on the details of the original fuel geometry; the overall density of the fuel within the cladding material

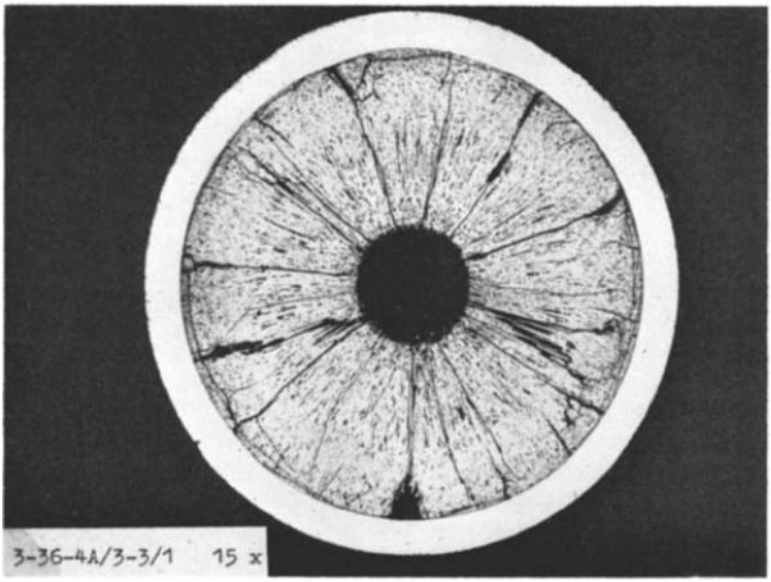

FIGURE 11. Cross section of a typical fuel pin showing central void and columnar grain structure.

is the controlling parameter. As this overall density takes into account not only the porous volume within the original pellets, but also the gap between pellet and cladding material, one speaks of the *smear density*. Smear densities between 80 and 85% of the theoretical fuel density are widely accepted (178). Such a low density gives enough space for the fission products to go into, particularly if the core operating conditions are high enough and therefore the mobility of fission products inside the fuel great enough. This is governed by the temperature profile, which depends for a given cladding temperature directly on the power output per centimeter pin length, the linear rod power, but in cylindrical geometry it does not depend on the radius of the pin. The generally accepted nominal, maximum linear rod power for UO_2/PuO_2 fuel today is always close to 450 W/cm (179). The fuel rating is dictated from fuel cycle economy considerations (16, 141) and is adjusted by the pin diameter (180). Again, a fuel rating close to 1 MW*t*/kg fiss for a 1000 MW*e* reactor and accordingly a pin diameter of 6 mm belong to these generally accepted specifications. The active core length is almost always close to 100 cm; above and beneath are breeding blankets of a size of 15–30 cm. The gradually building up fission gases are led to a plenum above or underneath either of the axial blankets. The thickness of the cladding is always close to 0.35 mm. The fuel pin design is summarized in Table 15.

In former years the specifications for fuel pins were largely a matter of experimental experience and judgment. Since 1967 or 1968 a more logical

TABLE 15. Characteristics of fast breeder reactor fuel pin

Smear density	80–85%
Max, midwall, hot spot clad temperature	700°C
Max linear rod power	450 W/cm
Fuel pellet diameter	6 mm
Thickness of clad	0.35 mm
Gap between fuel pellet and clad	80 μ
Type of clad	SS 16Cr13Ni
Active core length	100 cm
Size of upper and lower axial blanket	15–30 cm
Size of plenum	≈40 cm

and systematic approach has come to the forefront. It has been possible to establish mathematical models, crude in the beginning but constantly being refined (181, 182). The basic idea is to express the balance of the available volumes inside the pin. The porous volumes inside the fuel can accept fission products and these products are mobile according to the existing temperatures. A careful temperature assessment, taking into account the heat transfer in the cladding, the gap, and the temperature, density, and stoichiometry-dependent heat conductivity, is made. Some swelling of the fuel applies pressure to the cladding and originates tangential strains. Time to rupture is calculated by a creep analysis and the additional volume provided for by the creeping of the cladding enters the volume balance too. This analysis is applied to all (r,z) positions of the core. One interesting result is that the most dangerous point for fuel pin rupture is not the hottest point in the middle of the reactor, but a point somewhat underneath, where the flux is still high enough to create sufficient fission products and the temperature is already low enough to slow down the mobility of these products and thereby to inhibit their distribution to the principally available porous volume.

Lack of systematic experimental data is still typical because experiments of former years were largely on a trial and error basis and are of limited value for more generally applicable conclusions and because irradiation space with fast neutrons was very limited. The situation is gradually improving, however. This can be seen from the following: The main tool for fast-neutron irradiation in the US is still the EBR-II. As of July 1968, 105 fuel pins for test purposes were under irradiation there, all with UO_2/PuO_2 fuel coming from GE laboratories mainly, but also from NUMEC and PNL; 58 pins had been discharged at that time. As of August 1969, 86 of these 105 fuel pins were discharged and 48 additional pins have been inserted and their irradiation completed, giving a total of 134 discharged from EBR-II since July 1968. The majority of these pins have a burnup of 6% of all heavy (fissile and fertile) atoms. The present load with test pins in EBR-II (August 1969) is 118, of which 23 pins already have a burnup somewhat higher than 10%. GE and

PNL have seven subassemblies in with 37 pins each, thus providing a mass test; the burnups there as of August 1969 were ~1–3% (183).

The DFR loading with test pins is not so well published. In 1966 the irradiation of 14 pins was reported (184), but there is indication that perhaps 200 or 300 test pins of the British program have been irradiated to burnups in excess of 6%. The French fast-reactor program has obtained impressive irradiation results. The RAPSODIE reactor has started power operation with a fast flux of $\simeq 1.8 \cdot 10^{15}$ n/cm²sec since August 1967 and their whole first core with 2368 pins reached a maximum burnup of roughly 50,000 MWd/ton by the end of 1969 without major difficulties (185). This strongly confirms the above-described fast fuel pin concept. RAPSODIE will increase its flux to $3 \cdot 10^{15}$ with the RAPSODIE fortissimo version (186) and add an important irradiation tool. The German BENELUX fast-reactor program has up to now irradiated in the Belgian BR-2 and the British DFR. If the thermal component of the flux of the BR-2 is shielded away by a Cd-B flux shield, the remaining flux is still sufficient and fairly fast, which simulates the fast-reactor conditions (187); 9 pins have been irradiated there in excess of 5% burnup, 3 pins have reached a burnup in DFR of 6.0%, and a bundle of 39 pins in DFR reached a burnup of 4.2% by the end of 1969. During 1970 two subassemblies of 34 pins each will go into the RAPSODIE fortissimo reactor. In Karlsruhe there is the thermal-neutron, Na-cooled, 60 MW*t* KNK reactor which will be converted into the fast, 60 MW*t* KNK-II reactor by 1972 and thereby add fast-neutron irradiation space (188). For reasons of comparison, the Russian group reported in 1966 on their fast-neutron irradiations in BR-5, having a flux of $1 \cdot 10^{15}$. Up to 1965, 59 subassemblies with 80% PuO_2 and 21 subassemblies with 90% UO_2, each having 7 pins, had been irradiated, the PuO_2 fuel up to 4.2–6.5% and the UO_2 fuel to 0.96–1.4%. Since 1965 the BR-5 has had a carbide core and the irradiation of 580 pins was reported on (189). Of course all fast-reactor groups in the world did perform high burnup experiments in thermal test reactors, using as nearly as possible approximated fast-reactor pin conditions in order to provide a background for the more expensive fast-neutron irradiations.

Therefore one can conclude that by the end of 1970 there will be a satisfactory basis of irradiation experience with UO_2/PuO_2 fuel for the forthcoming 300 MW*e* prototype class. Because of that, most groups have gone into the development of high-performance fuel for fast reactors, mostly the carbides recently. In former years the limited irradiation experience with the carbides UC/PuC was not always encouraging (190). But with the improved understanding of the involved mechanisms and the help of the above-mentioned computer codes there is reason to believe in the success of the carbide development. But in spite of some early irradiations one has to say that the large and orderly approach for the development has started only recently. One incentive to convert to the carbides is the desire to attain high fuel ratings and thereby low first core inventories (191). A rating of 2 MW*t*/kg

fiss is a reasonable goal, which in turn means a flux of $1.3–1.4 \cdot 10^{16}$ n/cm²sec. Such fluxes are not available; only the future reactors FFTF in the US and the FR-3 in Germany have this potential, which in turn may indicate the time scale of the final performance testing of such fuel. Remember that the development and testing of the cladding material using such high-flux reactors would be on a completely different, much more inherently promising basis too.

Other Areas of Fast-Reactor Work

As this is a review paper the remaining areas of fast-reactor work will be touched briefly.

Fast-reactor safety.—Fast-reactor safety has been a subject for exploration from the beginning. Originally it was the short neutron lifetime that caused concern. But it is now clear that the short neutron lifetime is an advantage, provided the instantaneous power coefficient is negative. In that case the first power peak is terminated within a short time scale. One recalls that this time scale is given by $\sqrt{l/a}$, if l is the neutron lifetime and a the ramp rate. Also the inserted energy in that peak is smaller if the neutron lifetime is smaller, as this energy under the first peak is proportional to $\sqrt{l} \cdot a$ (77).

The second concern for fast-reactor safety stemmed from the EBR-I meltdown accident (192). A partial but instantaneous power coefficient, the bowing effects of fuel elements due to thermal gradients, was positive there. From that time on, attention has focused on the power coefficients. The phenomenon of the bowing effect became evident (193), but other coefficients came in with the second generation of fast breeders. As mentioned before the first was the Doppler coefficient. The role of the Doppler effect in an accidental sequence of events has not always been entirely clear. It is twofold: First, it terminates the first power peak of a fast excursion and decreases the energy that can be pumped into it and therefore gives time for the shutoff system to react. By the same token it helps to establish inherent operational stability. Second, it strongly influences the energy release figures of a Bethe-Tait calculation and makes these Bethe-Tait results less sensitive to the data of the equation of state of the involved reactor fuel (194, 195). This became apparent between 1962 and 1965.

The discussion of the partially positive Na void coefficient began in 1963 and is still going on, so far as its role in an accidental sequence of events is concerned. As mentioned before, such voiding of the inner core zones having positive Na void contributions really must take place. That requires either initiating reactivity ramp rates which can happen only if there is a complete failure of the shutoff system (it is debatable whether this is a reasonable assumption) or the blockage of a subassembly from the coolant flow. The latter can lead to Na ejection from this one subassembly. If the Na ejection is preceded by superheating of the fluid, concern exists that this ejection would be so violent that subassembly failure propagates to other subassem-

blies (196). In these cases and only in these cases is the Na void coefficient of significance (24). Depressing the Na void coefficient by distorting the cores, e.g. making them extremely flat to enhance leakage, hurts the breeding capability considerably and leads to the question whether it is reasonable to depress breeding through all the operation of a fast breeder because of accidents that are considered unrealistic. The situation is further complicated because the Bethe-Tait codes, which predict the accidental energy release, are essentially codes starting from a homogeneous core model. But the ejection of Na from cooling channels, which acts as kind of a ramp-rate multiplication (or initiation, respectively) makes reference to the pin-cooling channel geometry and is therefore a strong feature of heterogeneity. Because of this circumstance it is difficult to predict with real confidence the energy release of a Bethe-Tait event. Finally one has to realize that the after-meltdown decay heat of large 1000 MW*e* reactors is very great (10–100 MW*t*) and one has to remove it from a configuration that has experienced such a hypothetical accident. This requires active, engineered safeguard measures. If one goes into details, one realizes that active and therefore engineered safeguard measures are indeed unavoidable; if that is so, one should concentrate on avoiding Na ejection by such measures. These are among others the following: instrumentation of each subassembly in the core, diversification of the rods of the shutoff system, a second and completely independent and different shutoff system, avoidance of superheating by properly designed cooling channels and pin surfaces, and avoiding damage propagation from subassembly to subassembly by a proper design.

Logically compatible with the pronounced approach of engineered safeguards is the new discipline of reliability control. This has been developed in the field of electronics and the aerospace industry, where great numbers of identical or similar components are being used. The problem is whether these methods can be meaningfully transferred to reactor safety in general and fast-reactor safety in particular (197). The method consists in establishing fault trees of components, whose logical interconnection leads to the considered accident. One problem therefore is to establish functionally complete fault trees. Then it is necessary to have data on the failure rate of each of these components, and the method of handling the fault tree with a network type (critical path) of computer code finally arrives at a probability of the considered accident. The basic difference from former approaches to reactor safety is finally the quantification of risk in the framework of a systems-analysis approach. Today such analysis is applicable only to partial systems (198–203). Mathematical procedures of handling the fault tree have also been partially developed (204–207). A major problem is the collection of input data. The only way to do this is to evaluate statistics on operational experience (208–212). The final assessment of the merit of this approach is still under debate (213–216).

Heavy sodium components.—Mastering the Na technology requires first of all large and reliable Na pumps. Present Na reactors have pumps up to

3000 m^3/h(~12,000 gpm). The mechanical pump type now prevails; electromagnetic pumps are used today only for special purposes. Most 300 MW*e* prototype reactors will have pump sizes of 5000 m^3/h(~20,000 gpm), but present studies for pumps go far higher. There is general agreement that extended pump tests are required.

In addition to Na pumps, the steam generator requires special attention. Large Na-component test rigs must be built to develop and test these engineering components. The large 35 MW*t* Na-component test installation at Santa Susanna came into operation in 1965; in the UK the test rig for Na pumps came into operation in 1964/1965—these rigs provided the first significantly large test experience. Now larger test rigs are under construction in the US, Russia, France, the Netherlands, and Germany. It is with high confidence that one can expect the test results, which are necessary for the commitment on the construction of the 300 MW*e* prototypes. The attached Table 16 lists the more important and prototype-oriented test rigs.

All the existing fast breeder designs provide a primary and a secondary Na circuit and as a third circuit the steam-generating turbine circuit. Sometimes it was debated whether to leave out the intermediate circuit because of the related capital cost burden. Only recently has the Belgonucleaire of Belgium proposed a CO_2 gas turbine circuit as a second circuit, thus eliminating the intermediate Na circuit (217).

The Present Fast Breeder Reactor Projects

At present there are the following Na fast breeder projects:

1. In the USSR there is the BN-350 prototype reactor at the Kaspian Sea in the advanced stages of construction. This reactor is designed for 150 MW*e* and for 200 MW*e* equivalent for seawater desalination. The reactor is expected to be ready by the end of 1970. Construction of the 600 MW*e* BN-600 has just begun.

2. In Great Britain there is the PFR, a 250 MW*e* fast breeder prototype reactor, which is supposed to be ready by 1971.

3. In France there is the PHENIX reactor, a 250 MW*e* fast breeder prototype reactor, which will be ready by 1973.

4. In the US a study is going on by GE together with the ESADA group on a 310 MW*e* prototype plant; this reactor might go into operation by 1975. Westinghouse is conducting a similar study, also with utilities as partners; the contemplated size is 300 MW*e* and the reactor might also go into operation by 1975. Atomics International, together with the GPU group, is considering a 500 MW*e* plant; the time scale is similar to that of GE and Westinghouse.

5. Germany, together with Belgium, the Netherlands, and Luxembourg, is designing a 300 MW*e* SNR prototype plant. The construction will begin in 1971; 1975 is the date of completion. Germany's share is 70%, that of Belgium and the Netherlands 15% each.

6. In Japan a 200-300 MW*e* prototype is envisaged. It will be completed and ready for startup around 1976.

TABLE 16. Heavy sodium component test facilities

	Facility	Purpose	Technical data	Time schedule
USA	35 MW SCTI sodium component test installation	Testing of different steam generators and intermediate heat exchanger	Na-Na-steam system Na: max 650°C (700°C) Steam:560°C/170 atm	1965 Preoperational test 1966 Operation
	SPTF sodium pump test facility	Testing of pumps	Pump capacity up to 32,000 m³/h, temp max 650°C	1970 Construction 1972 Operation
USSR	3 MW sodium test loop	Investigation of steam generator and intermediate heat exchanger models		1960 Operation
	Sodium pump test facility	Testing of BN-350 pumps		1966 Construction
UK	Sodium pump test facility	Testing of sodium pumps	Pump capacity 1620 m³/h	1964/65 Operation
France	5 MW grand Quevilly	Investigation of steam generator and intermediate heat exchanger models	Na-NaK-steam system Na: max 600°C (625°C) Steam: 545°C (565°C)/130 atm	1964 Operation
	50 MW EDF test facility	Testing of steam generator	Na-steam system Na: max 650°C	1967 Construction 1970 Operation
Germany-BENELUX	5 MW INTERATOM test facility	Investigation of special aspects of steam generators	Na-Na-steam system Na: max 560°C Steam: 500–540°C/200 atm	1963 Construction 1965 Operation for KNK 1969 Operation for SNR
	INTERATOM sodium pump test facility	Testing of pumps	Pump capacity 5000 m³/h (15,000 m³/h)	1967 Construction 1970 Operation
	50 MW NERATOOM sodium component test facility	Testing of 50 MW steam generator and 70 MW intermediate heat exchanger	Na-Na-steam system Na: max 650°C Steam: 600°C/215 atm	1968 Construction 1970 Operation
Japan	2 MW sodium test facility	Investigation of various characteristics of sodium components	Na system, max 650°C	1969 Operation

Besides these prototype reactor projects the following projects are going on:

1. The SEFOR project achieved criticality in May 1969; it is a 20 MW*t* experimental reactor of SAEA, AEC, GE, and Karlsruhe together with EURATOM.

2. The FFTF project of the USAEC will be a 400 MW*t* test reactor; the expected neutron flux is $7 \cdot 10^{15}$ n/cm^2 sec and 6 big closed loops are envisaged.

3. Italy decided to build the PEC reactor, a 130 MW*t* test reactor; the expected neutron flux is $2.8 \cdot 10^{15}$ n/cm^2 sec and test loops are provided.

4. Interatom of Germany will convert the KNK reactor into the KNK-II reactor, a fast reactor with 20 MW*e*, 60 MW*t*. 1973 is expected to be the startup date for this KNK-II reactor; the thermal KNK reactor will go into operation by the end of 1970.

5. The BOR reactor of Russia is a test reactor with 60 MW*t*, which in a way is the extension of the BR-5 reactor line. Its date of startup was 1969.

6. A 100 MW*t* experimental fast reactor is under design in Japan. It is expected to go into operation by 1972.

7. India plans to build a 30-40 MW*t* experimental fast reactor of the French RAPSODIE type.

Concluding Remarks

Fast breeders have a strong and short-range economic incentive, particularly because the present generation of thermal power reactors produces large amounts of Pu, which can be used meaningfully only in fast breeders. And they have the long-range potential of breeding and therefore really making use of the existing uranium resources and more than that, of the ever-increasing vast amounts of depleted uranium (29, 30). Beyond the year 2000 breeding is a necessity and one should bear in mind that there are only 30 years left, that is, the lifespan of only one power station. Therefore there is no doubt that fast breeders are the ultimate solution of the problem of providing nuclear energy together with the achievement of very low nuclear energy production costs.

Acknowledgment

Many members of the fast-reactor team of Karlsruhe have provided information and contributions to this paper; we wish to express our sincere thanks to them all and particularly to R. Boehme, F. Helm, G. Karsten, G. Naegele, W. J. Oosterkamp, R. Schroeder, and D. Sellinschegg.

LITERATURE CITED

1. Wensch, G. W. 1966. In *Fast Reactor Technology: Plant Design*, ed. J. G. Vevick, p. 3. Cambridge, Mass: MIT Press
2. Yevick, J. G., 1966. See Ref. 1
3. *Directory of Nuclear Reactors.* 1960, 1962, 1966, 1968—3, 4, 6, 7. Vienna: IAEA
4. 1964. *Proc. 3rd Geneva Conf.* 6: *Fast Reactors*
5. 1965. *Fast Reactor Technol. Nat. Topical Meet., Detroit, ANS-100*
6. Philipps, J. L. 1965. *Nucl. Eng.* 10:264, 291
7. 1966. *Proc. London Conf. Fast Breeder Reactors.* London: Pergamon
8. 1967. *Fast Reactors Nat. Topical Meet., San Francisco, ANS-101*
9. 1957. *Proc. 1957 Fast Reactor Inf., Chicago, USAEC Rep.*
10. 1959. *Proc. Conf. Phys. Breeding, Argonne, ANL-6122*
11. Ergen, W. K., Zebroski, E. L. 1960. *Nucleonics* 18:No. 2
12. Sampson, J. B., Luebke, E. A. 1958. *Nucl. Sci. Eng.* 4:745
13. Greebler, P., Aline, P. 1959. See Ref. 10, *ANL-6122*, p. 116
14. Häfele, W. 1961. See Ref. 15, 3:601
15. 1961. *IAEA Seminar on the Physics of Fast and Intermediate Reactors, Vienna*
16. Cohen, K. P., Wolfe, B. 1963. *Nucl. News* 6:No. 2, 11
17. Greebler, P., Hutchins, B. 1961. See Ref. 15, 3:121
18. 1963. *Proc. Conf. Breeding, Economics and Safety in Large Fast Power Reactors, Argonne, ANL-6792*
19. Cohen, K. P. et al 1963. *APED-4281* and *8th Nucl. Congr., Rome*
20. Schnurr, W., Welsh, J. R. 1964. *3rd Geneva Conf. P/533*
21. Nims, J. B., Zweifel, P. F. 1959. *APDA-135*
22. USAEC 1964. *COO-279*
23. Mathiews, R. R. et al 1964. *3rd Geneva Conf. P/130*
24. Häfele, W., Smidt, D., Wirtz, K. 1965. See Ref. 25, *ANL-7120* pp. 162, 261. Smidt, D., Mueller, A. 1964. *Karlsruhe Rep. KFK-299*
25. 1965. *Proc. Conf. Safety, Fuels and Core Design in Large Power Reactors, Argonne, ANL-7120*
26. Peppler, W., Schlechtendahl, E. G., Schultheiss, G. F., Smidt, D. 1967. *Karlsruhe Rep. KFK-612*
27. Smidt, D., Fette, P., Peppler, W., Schlechtendahl, E. G., Schultheiss, G. F. 1968. *Karlsruhe Rep. KFK-790*
28. Schlechtendahl, E. G. 1969. *Karlsruhe Rep. KFK-1020*
29. Grümm, H. et al 1965. *Karlsruhe Rep. KFK-366*
30. Grümm, H. et al 1966. *Karlsruhe Rep. KFK-466*
31. Pittmann, F. K. 1963. Remarks presented at Fast Breeder Power Reactor Conf., Detroit
32. Cohen, K. P. 1967. Talk before ANS Nat. Topical Meet. Fast Reactors, San Francisco
33. Häfele, W. 1966. *Karlsruhe Rep. KFK-480*
34. Frame, A. G. et al 1966. See Ref. 7, p. 291
35. Carle, R. et al 1968. *Proc. Int. Conf. Sodium Technology Large Fast Reactor Design, Argonne, ANL-7520* 2:243
36. Harde, R. 1968. See Ref. 35, *ANL-7520* 2:130
37. Häfele, W. 1969. *Rep. Session of Fast Breeder Reactors, NUCLEX, Basel*
38. Leipunskij, A. I. et al 1969. *NUCLEX 1969. Basel, Tech. Meet. No. 4/5*
39. Astley, E. R. 1967. See Ref. 8 vol. 2. See also *BNWL-SA-978*
40. *BNWL FFTF Quart. Progr. Rep.* See especially 1968. *BNWL-880*
41. Leitz, F. et al 1967. See Ref. 8, *ANS-101* p. 7
42. Müller, A. et al 1966. *Karlsruhe Rep. KFK-392*
43. Häfele, W. 1969. *Atomwirtschaft* 14:190
44. Smidt, D. 1963. See Ref. 18, *ANL-6792*, p. 515
45. Fortescue, P. 1964. *3rd Geneva Conf. P/694*
46. Fortescue, P. 1969. *NUCLEX 1969, Basel, Tech. Meet. No. 4/6*
47. 1968. *ENEA Working Team on Fast Reactor Evaluation. An Assessment Study of Gas Cooled Fast Reactors for Civil Power Generation.* Confidential
48. Wirtz, K. 1965. *Karlsruhe Rep. KFK-359*
49. DalleDonne, M., Eisemann, E., Thümmler, F., Wirtz, K. 1969. *IAEA Proc. Conf. Advanced High Temperature Gas Cooled Reactors, Juelich*, p. 345

50. Fischer, M. 1969. *Karlsruhe External Rep. 8/69-7*
51. Aiello, P., Fogagnolo, G., Pierantoni, F., Zona, R. 1968. See Ref. 35, *ANL-7520* 2:269
52. Yuzo Endo 1969. *Nucl. Eng. Int.* 14:413
53. Power Reactor and Nuclear Fuel Development Corp. 1969. *PNC N141 69-14*
54. Goertzel, G. 1955. *1st Geneva Conf. P/613*
55. Nicholson, R. B. 1960. *APDA-139*
56. Hwang, R. N. 1965. *Nucl. Sci. Eng.* 21:523
57. Froelich, R. 1965. *Karlsruhe Rep. KFK-367*
58. Greebler, P., Goldman, E. 1962. *GEAP-4092*
59. Nordheim, L. W. 1964. In *Technology of Nuclear Reactor Safety* vol. 1. Cambridge, Mass: MIT Press
60. Nicholson, R. B., Fischer, E. A. 1968. *Advan. Nucl. Sci. Technol.* 4:109
61. Gast, K., Schlechtendahl, E. G. 1967. *Karlsruhe Rep. KFK-660*
62. Kato, W. Y., Butler, D. K. 1959. *Nucl. Sci. Eng.* 5:320
63. Baker, A. R., Jacques, T. A. J. 1958. *AERE R/M 168*
64. Fischer, G. J. et al 1963. See Ref. 18, *ANL-6792*, p. 885
65. Fischer, G. J. et al 1966. *Nucl. Sci. Eng.* 25:37
66. Till, C. E. et al 1969. *Proc. Int. Conf. Phys. Fast Reactor Operation and Design, BNES, London*, p. 40
67. Schröder, R. 1968. *Karlsruhe Rep. KFK-847*
68. Storrer, F. et al 1963. See Ref. 18, *ANL-6792*, p. 823
69. Fischer, E. A. 1969. *Karlsruhe Rep. KFK-844*
70. Baker, A. R., Collins, T. J. 1969. See Ref. 66, p. 213
71. Petersen, R. E., Newly, G. A. 1956. *Nucl. Sci. Eng.* 1:112
72. Billuris, G. et al 1967. See Ref. 8, *ANS-101*, pp. 5-31
73. Horst, K. M. et al 1967. See Ref. 8, *ANS-101*, pp. 5-31
74. Häfele, W., Cohen, P. K. et al 1964. *3rd Geneva Conf. P/644*
75. Caldarola, L. 1965. *Nulkeonik* 7:120
76. Ott, K. 1963. *Nukleonik* 5:285
77. Häfele, W. 1963. *Nukleonik* 5:201
78. Noble, L. D., Wilkinson, C. D. 1968. *GEAP-5576*
79. Weale, J. W. et al 1967. *Proc. IAEA Conf. Fast Reactor Physics, Karlsruhe* 2:533
80. McTaggart, M. H. et al 1967. See Ref. 79, 2:551
81. Meneghetti, D. 1966. *Proc. Int. Conf. Fast Critical Experiments and their Analysis, Argonne, ANL-7320*, p. 377
82. Wintzer, D. 1969. *Karlsruhe Rep. KFK-743*
83. Oosterkamp, W. J. 1969. *Karlsruhe Rep. KFK-1036*
84. Helm, F., Travelli, A. 1966. See Ref. 81, *ANL-7320*, p. 369
85. Karam, R. A. et al 1966. *ANS Winter Meet., Pittsburg, Pa. Trans. ANS* 9:No.2, 487
86. Pitterle, T. A., Yamamoto, M. 1967. *APDA-201*
87. Loewenstein, W. B. et al 1958. *2nd Geneva Conf. P/637*
88. Yiftah, S., Okrent, D., Moldauer, P. A. 1960. *Fast Reactor Cross Sections.* Pergamon
89. Toppel, B. J., Rago, A. L., O'Shea, D. M. 1967. *ANL-7318*
90. Gately, P. et al 1965. *AWREO-103*
91. Küsters, H., Metzenroth, M. 1965. See Ref. 25, *ANL-7120*, p. 423
92. Abagyan, L. P. et al 1964. Transl. in *Karlsruhe Rep. KFK-tr-144* (in German). New York: Russian Consultants Bureau
93. Küsters, H. et al 1968. *Karlsruhe Rep. KFK-793*
94. Greebler, P. et al 1966. *GEAP-4471*
95. Hummel, H. H., Rago, A. 1961. See Ref. 15, 1:231
96. Lewis, R. C. et al 1966. *NAA-SR-11980* vol. 3
97. Compilation of EANDC requests, 1966. *EANDC 55 "U"*
98. Honeck, H. C. 1966. *BNL-50066*
99. Chernick, J., Price, G., Levine, M. M. 1969. See Ref. 66, p. 77
100. Schmidt, J. J. 1966. *Karlsruhe Rep. KFK-120*
101. Langner, I., Schmidt, J. J., Woll, D. 1968. *Karlsruhe Rep. KFK-750*
102. 1969. *CCDN Newsletter Bull.* 11
103. Schomberg, M. G., Sowerby, M. G., Evans, F. W. 1967. See Ref. 79, 1:289
104. Gwin, R. et al 1969. *ORNL-TM-2598*
105. Pitterle, T. A. et al 1968. *Proc. Conf. Neutron Cross Sections and Technol. Washington*, p. 1243
106. Ribon, P. et al 1968. *CEA-N-989*
107. Schomberg, M. G. 1968. Unpublished
108. Ryabov, Y. V. et al 1968. *At. Energ.* 24:351
109. Broomfield, A. M. et al 1969. See Ref. 66, p. 40

110. Strutinsky, V. M. 1967. *Nucl. Phys.* A95:420
111. Schmidt, J. J. 1969. *Karlsruhe Rep. KFK-966*
112. Glass, N. H. et al 1968. See Ref. 105, p. 573
113. Beckurts, K. H. et al 1967. See Ref. 79, 1:67
114. Küsters, H. et al 1968. *Karlsruhe Rep. KFK-793*
115. Boeckhoff, K. H. et al 1966. See Ref. 126
116. Cao, M. G. et al 1968. See Ref. 105, p. 513
117. Yiftah, S. et al 1967. See Ref. 79, p. 123
118. Pitterle, T. A. 1968. *APDA-218*
119. Perkins, J. L. et al 1965. *J. Nucl. Energy* A/B 19:423
120. White, P. H. et al 1965. *J. Nucl. Energy* A/B 19:325
121. Davey, W. D. 1968. *Nucl. Sci. Eng.* 32:35
122. Poenitz, W. P. 1968. See Ref. 105, p. 503
123. White, P. H. et al 1965. *IAEA Conf. Phys. and Chem. of Fission, Salzburg* 1:219
124. Pfletschinger, E., Kaeppeler, F. *Nucl. Sci. Eng.* To be published
125. Garrison, J. D., Roos, B. W. 1962. *Nucl. Sci. Eng.* 12:115
126. Benzi, V., Bartolani, M. V. 1966. *Proc. IAEA Conf. Nucl. Data for Reactors, Paris* 1:537
127. Schröder, R. 1967. *Nukleonik* 10:18
128. Hoekstra, E. K. 1969. *RCN-111*
129. Huschke, H. 1968. *Karlsruhe Rep. KFK-770*
130. Kiefhaber, E. et al 1969. See Ref. 66, p. 94
131. Greebler, P., Hutchins, B. H., Linford, R. B. 1968. *Nucl. Appl.* 4:297
132. Barré, J. Y. 1968. *PNR/SETR R.026*
133. Broomfield, A. M. et al 1966. See Ref. 81, *ANL-7320*, p. 205
134. Travelli, A. 1966. See Ref. 81, *ANL-7320*, p. 481
135. Gasidlo, J. M. 1966. See Ref. 81, *ANL-7320*, p. 345
136. Broomfield, A. M., Palmer, R. G. 1968. *ANS Ann. Meet., Toronto. ANS Trans.* 11:No. 1, 203
137. Broomfield, A. M., Matloch, R. G., McVean, R. L. 1968. See Ref. 136, *ANS Trans.* 11:No. 1, 240
138. Davey, W. G. 1966. See Ref. 81, *ANL-7320*, p. 57
139. Greebler, P. et al 1967. *GEAP-5271*
140. Rowlands, J. 1969. See Ref. 66, p. 192
141. Häfele, W. 1963. See Ref. 18, *ANL-6792*, p. 265
142. Diehl, J. 1965. In *Moderne Probleme der Metallphysik* vol. 1. Berlin: Springer
143. Brinkmann, J. A., Wiedersich, H. 1965. *ASTM, Philadelphia, ASTM-STP-380*
144. Broomfield, G. H., Harries, D. R., Roberts, A. C. 1964. *AERE Rep. 4745*
145. Harries, D. R. et al 1964. *3rd Geneva Conf. P/162*
146. Harries, D. R. 1966. *J. Brit. Nucl. Energy Soc.* 5:74
147. Barnes, R. S. 1965. *Nature* 206:1307
148. Böhm, H., Dienst, W., Hauck, H., Laue, H. J. 1966. *J. Nucl. Mat.* 18:337
149. Böhm, H., Dienst, W., Hauck, H. 1966. *Karlsruhe Rep. KFK-445*
150. Böhm, H., Hauck, H., Hess, G. 1967. *J. Nucl. Mat.* 24:198. See also *Karlsruhe Rep. KFK-712*
151. Böhm, H., Hauck, H. 1969. *J. Nucl. Mat.* 29:184
152. Alter, H., Weber, C. E. 1965. *J. Nucl. Mat.* 16:68
153. Ljungberg, L. 1968. *4th Int. Conf. Radiation Damage in Structural Alloys, San Francisco*
154. De Pino, A., Jr. 1967. *Nucl. Appl.* 3:620
155. Cawthorne, C., Fulton, E. J. 1967. *Nature* 216:575
156. Bullough, R., Eyre, B. L., Perrin, R. 1969. *ANS Trans.* 12:No. 2, 523
157. Stiegler, J. O., Bloom, E. E., Weir, J. R. 1968. *ANS Trans.* 11:146
158. Holmes, J. J., Robbins, R. E., Brinhall, J. L., Mastel, B. 1968. *Acta Met.* 16:955
159. Holmes, J. J. 1969. *J. Nucl. Mat.* 29:241
160. Cunningham, G. W. 1968. See Ref. 153
161. Kulcinski, G. L., Mastel, B., Brinhall, J. L. 1969. *Radiat. Effects* 2:57
162. Lauritzen, T., Withop, A., Wolff, V. E. 1969. *Nucl. Eng. Design* 9:265
163. Böhm, H. et al 1969. *Karlsruhe Rep. KFK-985*
164. Laue, H. J. 1967. *Kerntechnik* 9:125
165. Fischer, M., Seetzen, J., Jansen, P., Faude, D. 1969. *Karlsruhe Rep. KFK-918*
166. Mastel, B., Brinhall, J. L. 1968. *BNWL-SA-1746*
167. Harkness, S. D. 1969. *ANL-7595*, p. 97
168. Claudson, T. T., Barker, R. W. 1969. *ANS Trans.* 12:No. 2, 524

169. Laue, H. J., Böhm, H., Hauck, H. 1968. *Karlsruhe Rep. KFK-814*
170. Laue, H. J., Closs, K. D., Guyette, M. 1969. *Karlsruhe Rep. KFK-1017*
171. Closs, K. D., Laue, H. J. 1969. *Karlsruhe Rep. KFK-1152*
172. Thorley, A. W., Tyzack, G. 1966. *Proc. IAEA Symp. Alkali Metal Coolants, Vienna*, p. 118
173. Weeks, R., Klamut, C. J., Gurinsky, D. H. 1966. See Ref. 172, p. 22
174. Böhm, H., Borgstedt, H. U., Rühle, M., Wincierz, P. 1968. *Plansee Seminar, Reutte, Tirol*
175. 1968. *4th Int. Conf. Radiat. Damage in Structural Alloys, San Francisco ASTM-STP-457*
176. 1969. *Proc. IAEA Symp. Radiat. Damage in Reactor Materials, Vienna*
177. Kämpf, H. 1967. In *Karlsruhe Rep. KFK-700*, No. 4
178. Karsten, G. 1967. In *Karlsruhe Rep. KFK-700*, No. 5
179. Karsten, G. 1968. *Karlsruhe Rep. KFK-878*
180. Benndorf, K. et al 1967. *Karlsruhe Rep. KFK-568*
181. Karsten, G., Kämpf, H. 1969. *ANS Trans.* 12:No. 2, 534
182. Bump, T. R. 1969. *ANS Trans.* 12:No. 2, 534
183. *ANL Reactor Development Program. Monthly Rep. July 1968-August 1969*
184. Lawton, H. et al 1966. See Ref. 7, p. 631
185. Gajac, G. et al 1968. See Ref. 35, p. 52
186. Ginier, R. et al 1969. *Proc. Int. Conf. Fast Reactor Irradiation Testing, Thurso, Caithness, Scotland*, p. 145
187. Karsten, G. et al 1969. See Ref. 186, p. 82
188. Plessa, G. 1969. See Ref. 186, p. 175
189. Leipunskij, A. I. et al 1966. See Ref. 7, p. 171. See also *ANS-100*, p. 121
190. Karsten, G. In *Karlsruhe Rep. KFK-1111*, No. 10
191. Jansen, P. 1970. *Karlsruhe Rep. KFK-1066*
192. Okrent, D. 1957. See Ref. 9, *Paper II-B*, p. 77
193. Storrer, F. 1961. See Ref. 15, 3:3
194. Wolfe, B. et al 1965. See Ref. 25, *ANL-7120*, p. 671
195. Braess, D. et al 1967. *CEA Conf. Fast Reactor Safety, Aix-en-Provence*
196. Smidt, D. et al 1965. See Ref. 25, *ANL-7120*, p. 33
197. Farmer, F. R. 1967. *IAEA Symp. Containment, Vienna, Paper SM-89/34*
198. Green, A. E., Bourne, A. J. 1966. *UKAEA Rep. AHSB(S)R.117*
199. Gieseler, H. 1966. *MRR 31*
200. Voigt, G. 1969. *5th Fachgespräch Inst. Reaktorsicherheit: Fortschr. Sicherheitsbeurteilung Kernkraftwerken, Hamburg.* 1970. *Rep. Inst. Reaktorsickerheit, Cologne, IRS-T18*
201. Mieze, G. 1969. See Ref. 200
202. Vendenberg, S. R. 1968. *GEAP-5653*
203. Weber, G. G., Heuser, F. W. 1970. *Proc. Ann. Conf. Reliability, Los Angeles*
204. Garrick, B. J., Gekler, W. C. 1967. *HN-190*
205. McKnight, C. W. *Na 66-838*
206. Woodcock, E. R. 1968. *UKAEA Rep. AHSB(S) R. 153*
207. Prochnow, D. 1969. *Kernenergie* 12:No. 4
208. Vetter, H. 1967. *Elektrizitätswirtschaft* 66:744
209. Green, A. E. *UKAEA Rep. AHSB(S) R. 164*
210. Mieze, G. 1969. *Rep. Inst. Reaktorsicherheit, Cologne, IRS-I 36*
211. Schlothauer, D. 1969. See Ref. 200
212. Ulken, D., Kuehl, H. See Ref. 200
213. Farmer, F. R. 1967. See Ref. 195
214. Farmer, F. R. See Ref. 200
215. Beattie, J. R. et al *UKAEA Rep. AHSB(S) R. 159*
216. Kellermann, O., Ullrich, U. 1969. *BNES Symp. on Safety and Siting, London*
217. Van Dievoet, J. P. 1968. See Ref. 35, 2:147
218. Pond, R. B., Till, C. E. 1969. *ANL-7410*, p. 87
219. Hummel, H. H. 1966. *ANL-7210*, p. 127